5-2014

Multidimensional CFD Modeling of a Liquid Salt Pebble Bed Heat Transfer Loop

Richard B. Cunningham
rcunnin6@utk.edu

To the Graduate Council:

I am submitting herewith a thesis written by Richard B. Cunningham entitled "Multidimensional CFD Modeling of a Liquid Salt Pebble Bed Heat Transfer Loop." I have examined the final electronic copy of this thesis for form and content and recommend that it be accepted in partial fulfillment of the requirements for the degree of Master of Science, with a major in Nuclear Engineering.

Arthur E. Ruggles, Major Professor

We have read this thesis and recommend its acceptance:

Graydon L. Yoder, Laurence F. Miller

Accepted for the Council:
Carolyn R. Hodges

Vice Provost and Dean of the Graduate School

(Original signatures are on file with official student records.)

Multidimensional CFD Modeling of a Liquid Salt Pebble Bed Heat Transfer Loop

A Thesis Presented for the
Master of Science
Degree
The University of Tennessee, Knoxville

Richard B. Cunningham
May 2014

Dedication

To my parents, Richard and Monica Cunningham, and my siblings: Kathryn, Michael, and Whitaker. Thank you for all of your love and support.

Acknowledgements

Thank you to Dr. Graydon L Yoder at Oak Ridge National Laboratory for his support and guidance during my undergraduate and graduate education. Also thank you to Dr. Arthur Ruggles at the University of Tennessee for his guidance in making this document.

Abstract

The Pebble Bed Advanced High Temperature Reactor (PB-AHTR) is a next generation reactor design proposed by the University of California at Berkeley. Oak Ridge National Laboratory's Liquid Salt Test Loop (LSTL) is designed to simulate AHTR operating conditions for component testing. In this study, COMSOL Multiphysics is used to model the LSTL. Full 3D modeling of the LSTL is computationally expensive. However, COMSOL allows users to combine 1D, 2D, and 3D fluid flow physics in order to design models that are both representative and efficient. 1D pipe flow calculations are used for the piping sections. COMSOL's porous media module is used with a 2D-axisymmetric geometry to model the fluid flow and heat transfer in the pebble bed core. The heat exchanger used to reject the loop energy to air was modeled using a 3D k-epsilon turbulence model. Modeling the LSTL in this manner requires 1D-2D and 1D-3D couplings using average operators on the 2D and 3D boundaries derived from the corresponding 1D boundary conditions. Using this strategy, a coupled model has been developed in COMSOL that provides CFD and heat transfer predictions for the LSTL. The model is presently being used to evaluate heat exchanger performance and determine potential loop operating points. The COMSOL results will be validated against experimental data once the loop is operating in 2014.

Table of Contents

List of Tables

List of Figures

Chapter 1 Introduction

1.1 Background

Liquid fluoride salts are desirable as high temperature energy system coolants due to low vapor pressure at high temperatures. This reduces the cost and complexity of the salt flow loop structures. In addition, fluoride salts offer high thermal conductivities and low corrosive effects when properly purified. Currently, there is no widely accepted high temperature energy transport fluid. Though many salts such as FLiNaK, FLiBe, and NaF-ZrF_4 have been researched for their thermophysical properties, very few have been experimentally studied in a liquid salt test loop featuring advanced reactor components. ORNL's Liquid Salt Test Loop (LSTL), shown in Figure 1, aims to experimentally test heat transfer properties of FLiNaK salt in a pebble bed flow channel and air-cooled heat exchanger. In addition to the pebble bed flow channel, the performance of various thermocouples, level detection devices, and a pressure transducer and flow meter will be tested with FLiNaK salt at temperatures up to 700 °C.

The LSTL has been constructed to support development of an FHR concept called the Pebble Bed Advanced High Temperature Reactor, designed by UC-Berkeley. The LSTL can operate up to 700 °C at a system pressure of about 30 psig. The LSTL pebble bed is heated by an induction coil, which is in turn powered by a 200 kW power supply. A forced flow, air-cooled heat exchanger removes heat from the system.

Figure 1. ORNL's Liquid Salt Test Loop.

1.2 Objectives and Requirements

This thesis develops a computational fluid dynamics (CFD) and heat transfer model of the LSTL that provides simulated results in a computationally non-intensive manner. Once the LSTL is running, these results will be benchmarked against the experimental data to confirm model performance. COMSOL Multiphysics was selected as the code to use for this modeling due to its capability to couple fluid computational

domains of different dimensionality. A full 3D model of the LSTL is unnecessary given that significant sections of the loop consist of piping and radially symmetric components. COMSOL's 1D Pipe flow module was used to calculate the velocity and pressure drop in the piping sections of the loop. For the pebble bed section, the Porous Media module was used to calculate a radially symmetric velocity profile and pressure profile through the bed. In the heat exchanger, the CFD module was used to run a full 3D k-epsilon turbulent flow simulation. These component simulations of dis-similar spatial dimensionality are coupled as an open loop system model. The integrated COMSOL model is compared to a 1D AFT Fathom pipe network model, and to hand calculations using standard engineering models. Component models for the pebble bed are also compared to legacy engineering models.

Chapter 2 Application

2.1 PB-ATHR

2.1.1 Design. The PB-AHTR is a high-temperature, high-efficiency, liquid salt cooled reactor design being developed at UC-Berkeley in collaboration with Oak Ridge National Laboratory and other DOE national laboratories. Due to its high power density of 20-30 MWth/m^3, the 900 MWth PB-AHTR core is about $1/10^{th}$ the volume of a 600MWth GT-MHR reactor vessel. This high power density is achieved by using 3-cm diameter graphite pebbles containing TRISO fuel, with a core outlet temperature of 700 °C.

The PB-AHTR design uses FLiBe salt as the primary coolant and FLiNaK salt as the intermediate coolant. FLiBe was selected as the primary coolant for its low parasitic neutron capture and high moderating capability, which allow for the design of a reactor core with a negative void reactivity. According to UCB calculations, FLiBe occupies 40% of the core volume and absorbs ~8% of the neutrons while also acting as an effective neutron moderator. FLiNaK was selected as the coolant for the intermediate loop, which carries energy to the helium working fluid of the Brayton cycle.

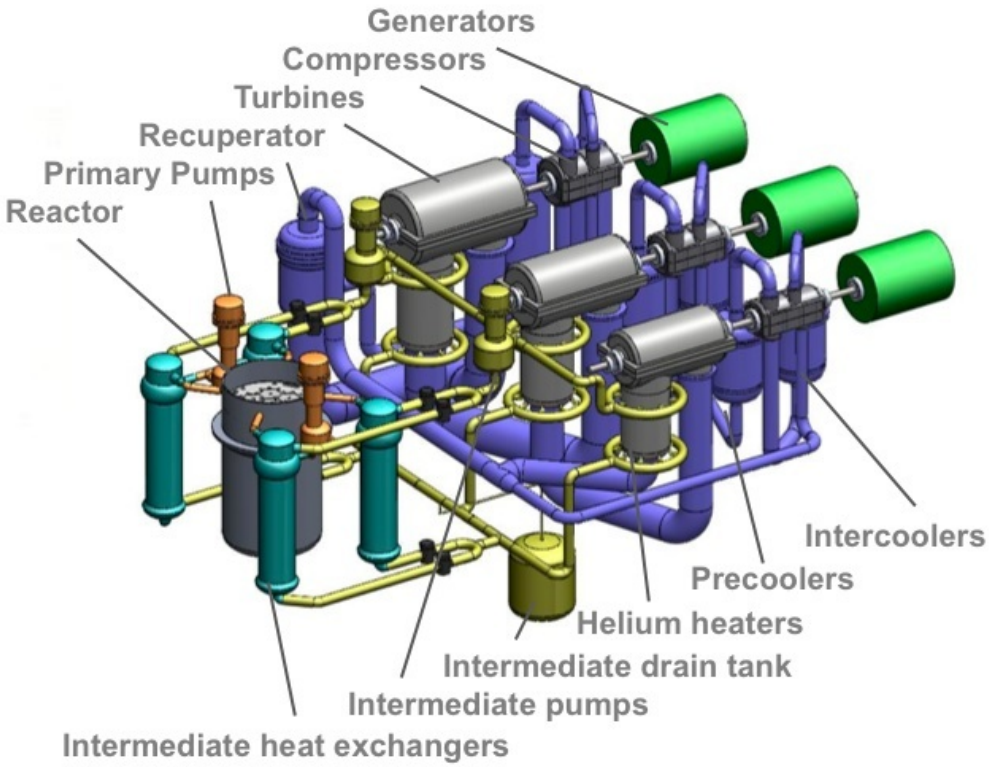

Figure 2. Power Conversion system for the PB-AHTR (Ref. 7).

Fuel pebble density is set at ~86% of the FLiBe salt operating density of 1.96 Kg/m^3 so that the pebbles will naturally float up to the top of the bed[7]. The top of the reactor core features a set of defueling chutes that collect the pebbles as they float up through the core. From here, the pebbles are either put back into the reactor through the bottom of the core or are discarded for storage or recycle depending on their burn-up. Due to high burn-up potential and power conversion efficiency, the PB-AHTR requires 70% of the natural uranium and 80% of the enrichment separative work needed for a typical PWR (Ref. 7).

2.1.2 Performance. The PB-AHTR achieves a 46% power conversion efficiency by using a multi-reheat Brayton cycle (Ref. 7), shown above in Figure 2. The reactor is capable of producing 410 MWe at full power, and is scheduled to run on 6-month cycles. Fuel pebbles are planned to run in a dual-cycle system, so that half of the pebbles in the core are fresh and half are on their second 6-month cycle.

The PB-AHTR has passive safety systems for reactivity control and decay heat removal. Classical forced shutdown rods as well as buoyancy-force driven shutdown rods are used to control reactivity in an off-normal event. The core's low excess reactivity and intrinsic negative coolant and fuel temperature reactivity feedback aid the shutdown rods in system control. Normally, shutdown heat removal is performed by the intermediate heat transfer loop (FLiNaK). However, a passive Direct Reactor Auxiliary Cooling System (DRACS) is also available. The DRACS features an air-cooled chimney style natural circulation heat exchanger to reject decay heat during an off-normal event. After a loss of on-site pumping power, flow through the reactor core slows and eventually reverses in the DRACS by way of natural circulation. A vortex flow diode on the DRACS leg allows natural circulation to be the driving force for heat rejection without active system intervention, while minimizing parasitic heat loss during normal operation. The PB-AHTR plant design with reactor core, DRACS, and power conversion system is shown in Figure 3.

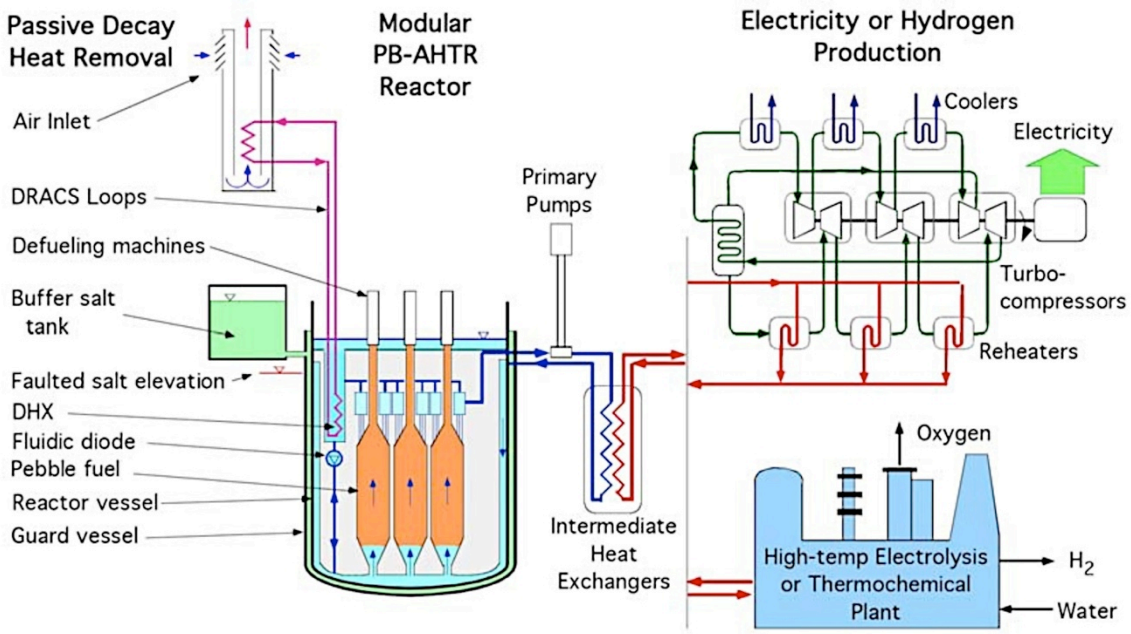

Figure 3. PB-AHTR Power Plant Design (Ref. 7).

2.2 Liquid Salt Test Loop

2.2.1 Design. ORNL's Liquid salt test loop features an inductively heated graphite pebble bed flow channel and air-cooled heat exchanger. The randomly packed pebble bed contains 3 cm diameter graphite spheres that simulate the heat transfer of graphite fuel pebbles. An induction heating coil was selected as the heating source in order to facilitate the desired nuclear fuel heat generation properties. The pebble bed housing is a 72 cm x 15 cm diameter Silicon Carbide (SiC) cylinder, chosen for its transparency to the electromagnetic (EM) field produced by the induction coil. The graphite spheres are heated by the EM field and exhibit heat generation characteristics similar to PB-ATHR fuel. FLiNaK was selected as the loop coolant in order to obtain experimental computational fluid dynamics (CFD) and heat transfer (HT) data for the

secondary coolant in the PB-AHTR design, while avoiding safety issues associated with the use of Beryllium. A loop schematic is shown below in Figure 4.

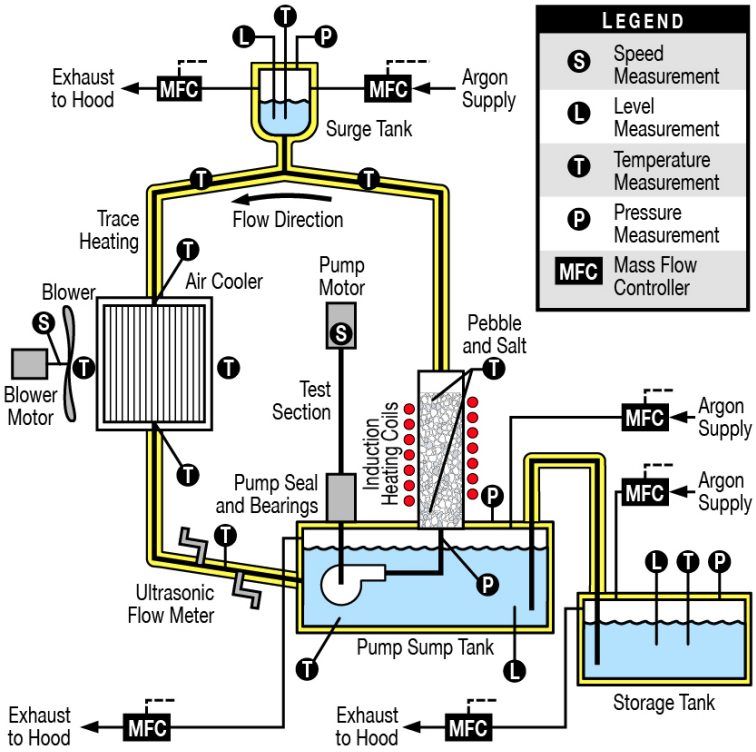

Figure 4. Schematic of ORNL's Liquid salt test loop (Ref. 3)

Loop cooling is supplied by an air-cooled finned tube heat exchanger designed to reject the 200 kW of heat load into the system by the induction coil. Loop pressure is maintained by an Argon cover gas supply system. All 3 salt tanks have independent cover gas supply's that are used to fill and pressurize the loop prior to pump startup. A surge tank at the top of the loop allows the loop to be completely filled without the threat of bubbles in the system and establishes system pressure during operation.

Trace heating and thermal insulation is applied on all piping sections of the loop to ensure that the loop temperature remains above the FLiNaK melting temperature of 454°C. The storage, sump, and surge tanks are encapsulated in custom heater blankets that also serve as thermal insulation. The heat exchanger upper and lower tanks are heated by tubular resistance heating elements to eliminate cold spots. Sliding doors at the heat exchanger air inlet and outlet allow the 14 finned tubes to be heated, also with tubular heating elements, above the FLiNaK melting temperature.

Salt will be purified in a Nickel crucible located near the loop by bubbling HF gas to remove water, oxygen, and other impurities. Once melted and purified in the crucible, salt is transferred through a Nickel tube to the storage tank, which serves as long-term salt storage. To fill the loop, all trace heating and heating blankets must pre-heat the entire loop. The storage tank can then be pressurized to push salt into the sump tank. While holding pressure in the storage tank, the sump tank is then pressurized to push salt into the loop. At that point the storage tank is isolated, the surge tank is pressurized to hold the salt level steady, and the loop is ready for operation by starting the pump and applying power to the induction coil.

2.2.2 Performance. The centrifugal, vertical shaft driven pump is designed to provide an operating mass flow rate of 4.5 Kg/s. This flow rate is based on simulating conditions in the PB-AHTR. Matching the pebble Reynolds number ensures that the heat transfer and fluid flow conditions in the LSTL are representative of the PB-ATHR:

$$Re_p = \frac{\rho v_s D_p}{\mu}$$

where,

$$\rho = salt\ density$$

$$v_s = superficial\ bed\ velocity$$

$$D_p = pebble\ diameter$$

$$\mu = salt\ viscosity$$

The PB-AHTR design uses the same diameter pebbles (3 cm) as those in the LSTL. Reactor operating conditions are 700°C and a superficial bed velocity of 35 cm/s with FLiBe salt (ρ = 1940 Kg/m^3, μ =6.78x10^{-3} Pa-s). This results in a pebble Reynolds number of 3100.

Dependent on factors such as loop size and cost, it was determined that the LSTL pebble Reynolds number did not need to exactly match that of the PB-AHTR, but instead only be above the Reynolds critical number for turbulent, developed flow (Re = 2000). The pebble Reynolds number for the LSTL was then set to Re_p = 2600, which corresponds to the mass flow rate previously referenced.

Pebble bed void fractions are greatly affected by the ratio of bed diameter to pebble diameter. Pebble packing is limited at the wall surface, resulting in an increased void fraction. The non-dimensional length scale D* is used in evaluating the effect of the bounding wall, defined:

$$D^* = {D_b}/{D_p}$$

where,

$$D_b = bed\ diameter$$

$$D_p = pebble\ diameter$$

Studies have shown that when D* is greater than 25 the void fraction at the center of the bed is no longer impacted by the wall effect. For the PB-AHTR, D* is approximately 6.7, indicating that the pebble bed centerline is greatly affected by the wall. D* for the LSTL, therefore, could be much less than 25 and still provide an accurate simulation of the PB-AHTR core. In order to minimize the required flow through the pebble bed, a bed diameter of 15 cm was selected for the LSTL. This corresponds to a D* value of 5, which is very close to the PB-AHTR D* value of 6.7.

The induction coil is designed to apply a maximum of 1285 W/pebble (peak), the same as the PB-ATHR. Assuming a total power input to the pebble bed of 150 kW, a fluid ΔT of 20°C is expected through the pebble bed. At steady state, the same amount of heat is expected to be rejected in the heat exchanger, resulting in a ΔT of -20°C. The table below shows the expected pressure and temperature values at various points in the LSTL. Locations listed in Table 1 are shown in Figure 5.

Table 1. Expected loop pressure and temperature characteristics

Location	***Pressure, psig***	***Temperature, °C***
Pump discharge	29.8	680
Test section outlet	21.8	700
Surge tank liquid level	15.0	700
Heat exchanger inlet	15.3	700
Heat exchanger outlet	12.7	680
Pump suction	8.1	680
Sump liquid level	7.2	680

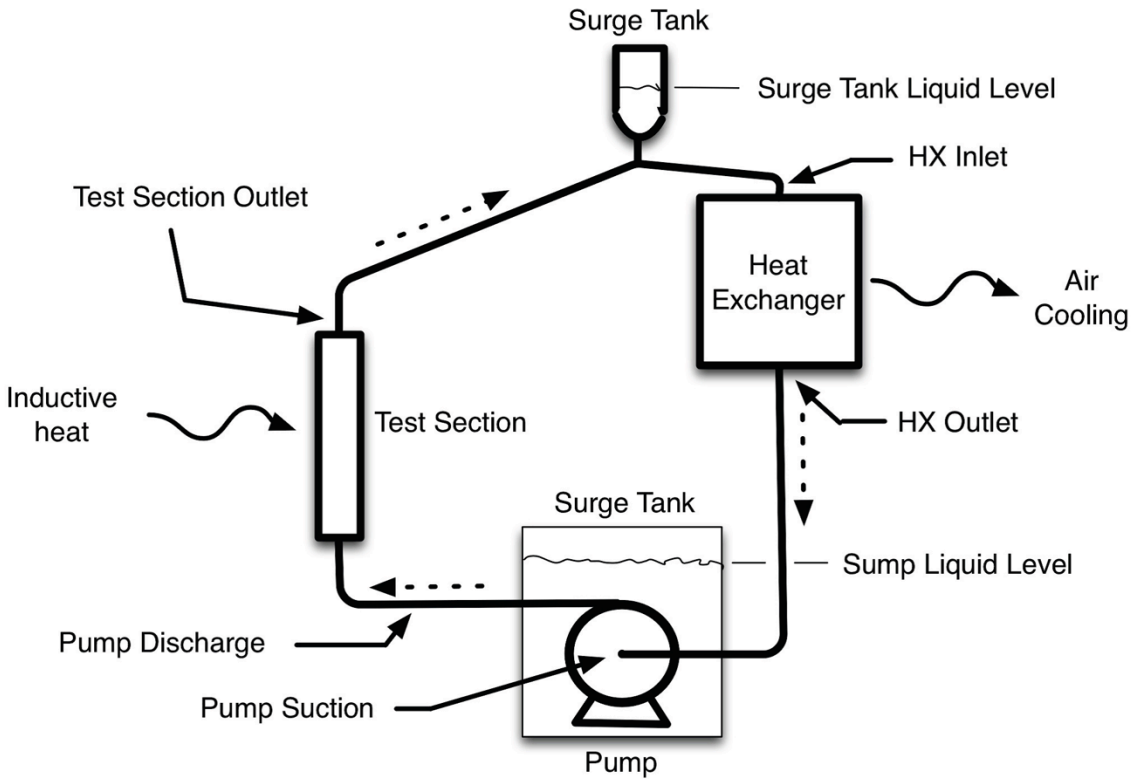

Figure 5. LSTL schematic depicting locations listed in Table 1.

Chapter 3 Theory

3.1 1D-3D Coupling

3.1.1 Velocity Profile Mismatch. 1D to 3D couplings occur at the heat exchanger inlet and outlet. In the 1D pipe flow sections, the fluid has a uniform velocity profile. In the 3D turbulent flow sections, the fluid is approximated with a $1/7^{th}$ power law velocity profile $\left(\mathrm{Re} = 7.8\times10^{4}\right)$, defined:

$$v(r) = \left(1 - \left(r/R\right)\right)^{1/7} v_{cL}$$

where
r = local radius
R = tube radius
v_{cL} = centerline velocity

At the 1D-3D interface, the fluid velocity profile must make a transition from a constant velocity to the radially dependent power law profile shown above. This velocity profile mismatch causes a momentum and energy difference across the transition. Mass flow across the interface is assumed to be constant for the momentum and energy evaluation. Using Reynolds Transport Theorem (RTT), this difference can be quantified. RTT is shown below

$$\frac{d}{dt}\iiint_V \rho c\, dV + \iint_S \rho c\vec{v}\cdot\hat{n}\, dS = \iiint_V \rho\phi\, dV + \iint_S \vec{J}\cdot\hat{n} dS$$

mass: $\mathrm{c} = 1, \vec{\mathrm{J}} = 0, \phi = 0$

momentum: $\mathrm{c} = \vec{v}, \vec{\mathrm{J}} = \bar{\bar{\tau}} - P\bar{\bar{I}}, \phi = \vec{g}$

energy: $\mathrm{c} = u + \frac{v^2}{2}, \vec{\mathrm{J}} = q'' + (\bar{\bar{\tau}} - P\bar{\bar{I}})\cdot\vec{v}, \phi = q'''/\rho + \vec{g}\cdot\vec{v}$

The change in pressure from the 1D outlet to the 3D inlet is found by performing a momentum balance at the interface. With the mass balance assumed exact, the 1D flow velocity is given as:

$$\int_0^r \left(1-\left(r/R\right)\right)^{1/7} \rho 2\pi r dr = \pi r^2 \rho \bar{v}$$

The 1D momentum then causes a mis-representation of the 3D momentum, which can be expressed as a pressure defect,

$$\Delta P = \rho \bar{v}^2 - \int_0^r \left[\left(1-\left(r/R\right)\right)^{1/7}\right]^2 \rho 2\pi r dr$$

This defect is evaluated as 599 Pa for $\bar{v} = 3.96$ m/s.

Similary, an energy mismatch is found at the interfaces, where internal energy is lost from 3D to 1D, and gained from 1D to 3D due to velocity and temperature profile averaging followed by reconstruction. The energy mismatch results in a Δu of 2.7 J/Kg for ΔP = 599 Pa and $\bar{v} = 3.96$ m/s. These momentum and energy mismatches will occur at the 1D-3D and 3D-1D interface as a result of products of averages not being equal to averages of products. This assessment offers representative values for errors introduced by these approximations.

Chapter 4 Computational Modeling

4.1 CFD

4.1.1 Pipe Flow. The 1D Pipe Flow module in COMSOL allows users to model pipe flow sections in a simple and efficient manner. COMSOL calculates the pressure and velocity of an incompressible fluid by solving applicable continuity and momentum equations. For this model, 1D pipe flow calculations are performed on lines drawn in the 3D model window. These lines represent the pipe flow sections, and are assigned pipe characteristics such as diameter, wall thickness, etc. Figure 7 shows the pipe flow locations before and after the heat exchanger and pebble bed. The momentum and continuity equations for pipe flow (Ref. 1) are given below:

$$\text{Momentum: } \rho\frac{\partial u}{\partial t} = -\nabla p - f_D\frac{\rho}{2d_h}u|u| + F$$

$$\text{Continuity: } \frac{\partial A\rho}{\partial t} + \nabla\cdot(A\rho u) = 0$$

Here, u is the cross section averaged velocity, p is pressure, f_D is the Darcy friction factor, and F is a volume force term. d_h is the hydraulic diameter, given by

$$d_h = \frac{4A}{P_{wet}}$$

$d_h = d$ (cylindrical pipes)

where A is the cross sectional area available for flow, P_{wet} is the wetted perimeter, and d is the cylindrical pipe diameter. For the 1D pipe flow calculation, a tangential unit vector, e_t is used for direction in the momentum equation.

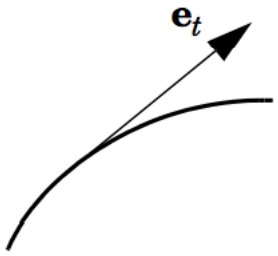

Figure 6. Unit tangent vector to pipe axis.

e_t is defined by x, y, and z components:

$$\mathrm{e}_t = \left(e_{t,x}\ e_{t,y}\ e_{t,z}\right)$$

All velocity components normal to the pipe axis are assumed to be zero, so the momentum balance can be rewritten:

$$e_t \cdot \left[\rho \frac{\partial u}{\partial t} = -\nabla p - f_D \frac{\rho}{2d_h} u|u| + F\right]$$

The tangential velocity can now be defined as $\boldsymbol{u} = ue_t$ and the volume force $\boldsymbol{F} = Fe_t$, so the momentum balance can be rewritten in the steady-state form:

$$0 = -\nabla p - f_D \frac{\rho}{2d_h} \boldsymbol{u}|\boldsymbol{u}| + \boldsymbol{F}$$

The tangential velocity u is the quantity the user defines for an inflow boundary condition, and the quantity that COMSOL solves for along the pipe edge. COMSOL

makes the following assumptions in the pipe flow calculation (COMSOL Multiphysics 2013) :

- The velocity profile is fully developed and does not change within a section
- The cross section area is allowed to change between pipe segments
- Empirical functions describe viscous losses
- Shocks are neglected (low Mach number incompressible flow)
- The flow direction is in the direction of the pipe axis

The Darcy friction factor, f_D , accounts for pressure drop due to viscous shear along a pipe length. The Darcy friction factor is a function of Reynolds number and the surface roughness divided by the hydraulic diameter:

$$f_D = f_D\left(\mathrm{Re}, \frac{e}{d_h}\right)$$

where

$$\mathrm{Re} = \frac{\rho u d_h}{\mu}$$

Surface roughness values are predefined for a set of materials in the user interface, and can also be manually entered for other materials. The Churchill equation (shown below) was selected to calculate f_D in COMSOL because it is acceptable in all ranges of Reynolds numbers: laminar, transitional, and turbulent.

$$f_D = 8\left[\left(\frac{8}{\mathrm{Re}}\right)^{12} + (A+B)^{-1.5}\right]^{1/12}$$

where A and B are defined:

$$A = \left[-2.457\ln\left(\left(\frac{7}{\mathrm{Re}}\right)^{0.9} + 0.27\left(e/d\right)\right)\right]^{16}$$

$$B = \left(\frac{37530}{\mathrm{Re}}\right)^{16}$$

Minor losses such as bends, valves, junctions, contractions, and expansions are added as point conditions between pipe segments in the Pipe Flow Module. These losses are responsible for abrupt pressure drops in their locations. Pressure drop is calculated:

$$\Delta p = \frac{1}{2} K_f \rho \boldsymbol{u}^2$$

Loss coefficients, K_f, are predefined in the COMSOL Pipe Flow user interface and can be found on page 39 of Ref. 6. Figure 7 shows the edges where the 1D pipe flow calculation is performed in a 3D geometry.

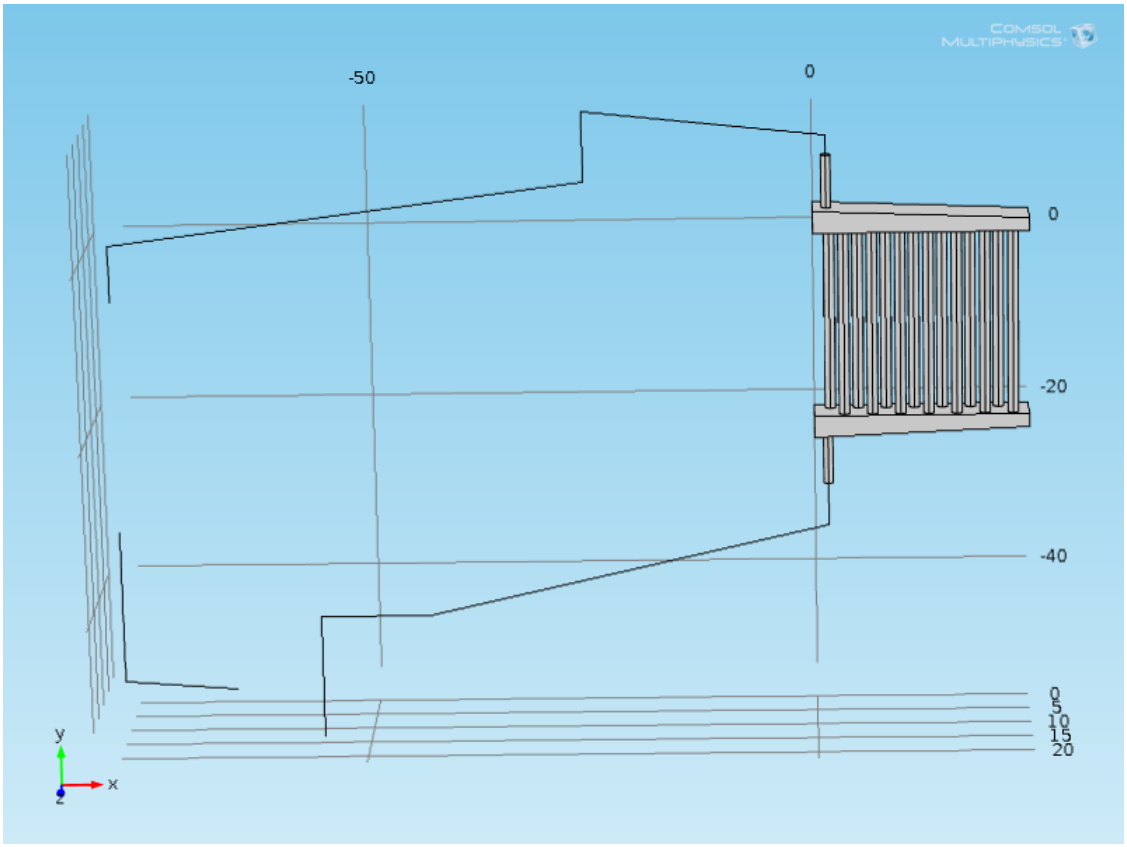

Figure 7. LSTL model geometry showing 1D pipe flow lines.

4.1.2 3D Turbulent Flow. The 3D flow physics are based on the general Navier-Stokes equations for mass, momentum, and energy:

$$\text{mass: } \frac{\partial \rho}{\partial t} + \nabla \cdot (\rho \boldsymbol{u}) = 0$$

$$\text{momentum: } \rho \frac{\partial \boldsymbol{u}}{\partial t} + \rho (\boldsymbol{u} \cdot \nabla) \boldsymbol{u} = \nabla \cdot [-p\boldsymbol{I} + \tau] + \boldsymbol{F}$$

$$\text{energy: } \rho C_p \left(\frac{\partial T}{\partial t} + (\boldsymbol{u} \cdot \nabla) T \right) = -(\nabla \cdot \boldsymbol{q}) + \tau : \boldsymbol{S} - \frac{T}{\rho} \frac{\partial \rho}{\partial T}\bigg|_p \left(\frac{\partial p}{\partial t} + (\boldsymbol{u} \cdot \nabla) p \right) + Q$$

The fluid is assumed Newtonian, so the viscous stress tensor, τ, becomes:

$$\tau = 2\mu \mathbf{S} - \frac{2}{3}\mu (\nabla \cdot \mathbf{u}) \mathbf{I}$$

where **S** is the strain-rate tensor

$$\mathbf{S} = \frac{1}{2}\left(\nabla\mathbf{u} + (\nabla\mathbf{u})^T\right)$$

Under the Newtonian fluid assumption, the dynamic viscosity, μ, is dependent on the thermodynamic state but not on the velocity field. Temperature-dependent viscosity values are used in this COMSOL model from Ref. 2.

At the wall boundary, a no-slip condition is assumed, which leads to the development of the velocity profile due to wall shear. The fluid velocity at the wall is zero:

$$\mathbf{u}_w = 0$$

The k-ε turbulence model introduces two additional transport equations and two dependent variables: the turbulent kinetic energy, k, and the dissipation rate of turbulence energy, ε. The turbulent kinetic energy is defined:

$$k = \frac{3}{2}(U_0 I_T)^2$$

where

U_0 = velocity magnitude
I_T = turbulent intensity

The dissipation rate of turbulence energy is defined:

$$\varepsilon = C_\mu^{3/4}\frac{k^{3/2}}{L_T}$$

where

$C_\mu = 0.09$ (modeling constant)
L_T = turbulent length scale

Turbulent intensity and length scale are both variables requiring an input for the k-ε model. The turbulent length scale is a physical quantity describing the size of the large energy-containing eddies in a turbulent flow. The turbulent length scale can be estimated for fully developed pipe flow based on hydraulic diameter:

$$L_T = 0.038 d_h$$

For the heat exchanger, the hydraulic diameter at the inlet is 0.0254 m.

Turbulent intensity is the ratio of the root-mean-square of the turbulent velocity fluctuations to the mean velocity of the flow. For fully developed pipe flow, turbulence intensity is estimated to be (Ref. 14):

$$I_T = 0.16 \times \mathrm{Re}^{-1/8}$$

4.1.3 2D-axisymmetric Porous Media. There are a few different ways to model the pebble bed section of the Molten Salt Loop in computational fluid dynamics. For this experiment, the Porous Media module was used in COMSOL. The Porous Media module allows the user to input porosity and permeability data into the geometry of interest. This greatly reduces the complexity of the problem and significantly cuts down on computational time. Because the geometry of interest is a cylinder, a 2D-axisymmetric geometry was used in COMSOL. Another option is to build a full-scale 3D model and treat the pebble bed as a turbulent flow channel. Running a full 3D model is quite computationally intensive and is also difficult to model geometrically. In order to accurately model a randomly packed bed, a high quality CT scan of the existing pebble bed would be required to extract a 3D CAD model and feed into COMSOL. Another issue with this approach is obtaining and knowing how to use imaging software that is

accurate enough build the 3D geometry correctly. Very small tolerances are required at pebble-pebble and pebble-wall contact points to correctly model the flow fields around the pebbles themselves.

4.2 Heat Transfer

4.2.1 Pebble Bed. Heat transfer in the pebble bed is modeled using COMSOL's 'Heat Transfer in Porous Media' function in the porous media module. The pebble bed channel wall is assigned a zero heat flux (thermal insulation) term, so that heat only leaves the pebble bed through the outlet. The thermal insulation term is detailed below.

$$-n \cdot \left(-k \nabla T\right) = 0$$

n = directional term
k = thermal conductivity
∇T = temperature gradient

Because the heat source for the pebble bed is an induction coil known to deliver 200 kW to the pebbles, a total power heat source was selected in COMSOL. This heat source is detailed below

$$Q = \frac{P_{tot}}{V}$$

Q = volumetric heat term
P_{tot} = total power
V = volume

P_{tot} was assigned 200 kW, and COMSOL calculated the volumetric heat term based on the pebble bed volume. Heat transfer in the pebble bed is modeled by the energy balance

below, which has a convection term on the left side, and conduction and power terms on the right side.

$$\rho C_p u \cdot \nabla T = \nabla \cdot \left(k \nabla T \right) + Q$$

ρ = density
C_p = specific heat
u = fluid velocity

The porous media module then solves this equation with temperature-dependent properties to find the steady state solution. LSTL inlet temperature is set at 680 °C.

4.2.2 Heat Exchanger Tubes. The heat exchanger on the LSTL removes heat from the system by having fluid flow through the heat exchanger tubes. These tubes have finned outer walls with a loop design volumetric flow of 2.77 m^3/s of air flowing around them. Heat is rejected from the fluid through the heat exchanger tube wall and transferred to the outside moving air. Because the finned tube walls would be quite complex to build and model in COMSOL, a representative heat transfer coefficient is calculated and applied to the outer tube wall. The heat transfer coefficient is calculated from a Nusselt correlation in Table 6.4 from Ref. 10. The correlation is based on staggered tube bundles with helical fins. A Reynolds number is calculated for air flowing through the tube bundle using tube diameter, d, and the velocity in the narrowest cross section between neighboring tubes, found to be 14.4 m/s. This yields a Reynolds number of 23,500 which corresponds to the Nusselt correlation in the Appendix. The Nusselt correlation results in a Nusselt number of 93.85. Using $\mathrm{Nu}=\frac{hd}{k}$, a heat transfer coefficient can now be calculated. For the tube bundle, d = 0.0254 m, and for air, k =

0.0257 W/m*K. Applying these values yields a surface heat transfer coefficient of 81.04 W/m^2*K. However, this heat transfer coefficient is based on the total fin surface area of 7.49 m^2. The total surface area of the heat exchanger tubes in the LSTL model is 0.559 m^2. Re-calculating the heat transfer coefficient to be dependent on tube surface area results in a value of 1,086 W/m^2*K.

Now that a heat transfer coefficient has been calculated, it is assigned to the tube outer walls in the heat exchanger, shown in Figure 8.

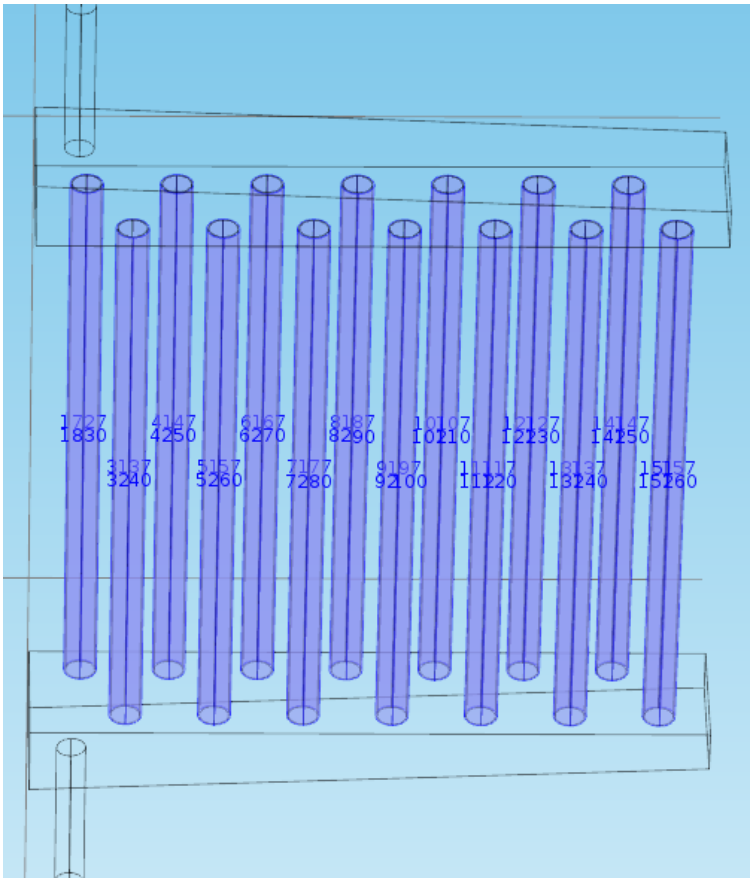

Figure 8. Heat transfer coefficient applied to outer walls of heat exchanger tubes.

The assigned heat flux is dependent on a heat transfer coefficient and temperature difference between the external bulk temperature and surface temperature of the tube wall.

$$q = h \cdot \left(T_{ext} - T \right)$$

For the LSTL, the bulk air temperature is 20 °C. This heat flux assignment is responsible for all of the heat transfer in the heat exchanger.

Modeling heat transfer due to radiation is outside the scope of this model simulation. In order to model radiation heat transfer, the air duct and finned tubes need to be modeled. An estimate of the radiation heat transfer is calculated using

$$q'' = \varepsilon \sigma \left(T_h^4 - T_c^4 \right)$$

ε = emissivity of object
$\sigma = 5.6703 \times 10^{-8} \left(W / m^2 K^4 \right)$ (Stefan-Boltzmann Constant)
T_h = temperature of hot object (K)
T_c = temperature of cold object(K)

Assuming the tubes are not finned, the tube surface temperature is 650 °C, the air duct enclosure walls are 50 °C, and they completely surround the heat exchanger tubes, then the radiation heat transfer from the heat exchanger tubes to the duct walls is about 35.6 kW/m^2. The tubes see the radiation from one another, so this will over estimate the outcome. Dividing q'' by ΔT = 600 °C results in a radiation effective heat transfer coefficient of 59 W/m^2-K. The fins make this evaluation much more challenging, as they are absorbing, re-radiating, and convecting.

4.3 Meshing

4.3.1 Pebble Bed. The pebble bed is modeled as porous media in a 2D radial geometry and meshed using COMSOL's default mesh settings with added boundary layers at the silicon carbide wall. The default 'coarser' setting was used, as this is the finest mesh that allows the coupled model to converge. Independent studies of pebble bed mesh refinement have shown that finer meshes do not have a significant impact on results. Therefore, the 'coarser' mesh setting is a compromise that yields acceptable results while avoiding a convergence issue. The pebble bed mesh consists of 1,939 elements and is shown in Figure 9.

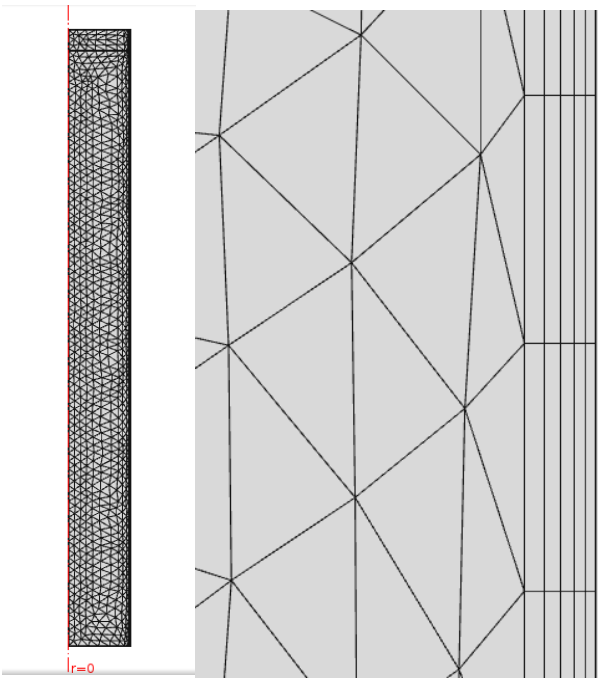

Figure 9. Pebble bed mesh using COMSOL's 'coarser' mesh setting (left) and a blown up view of mesh boundary layers (right).

4.3.2 Piping. Piping sections of the LSTL are modeled using COMSOL's pipe flow module. Meshing was adjusted in order to have nodes every 1.5" in the piping. Because the pipe flow module only uses simple 1D loss calculations, this part of the LSTL mesh adds minimal degrees of the freedom to the model. The piping mesh is shown in Figure 10.

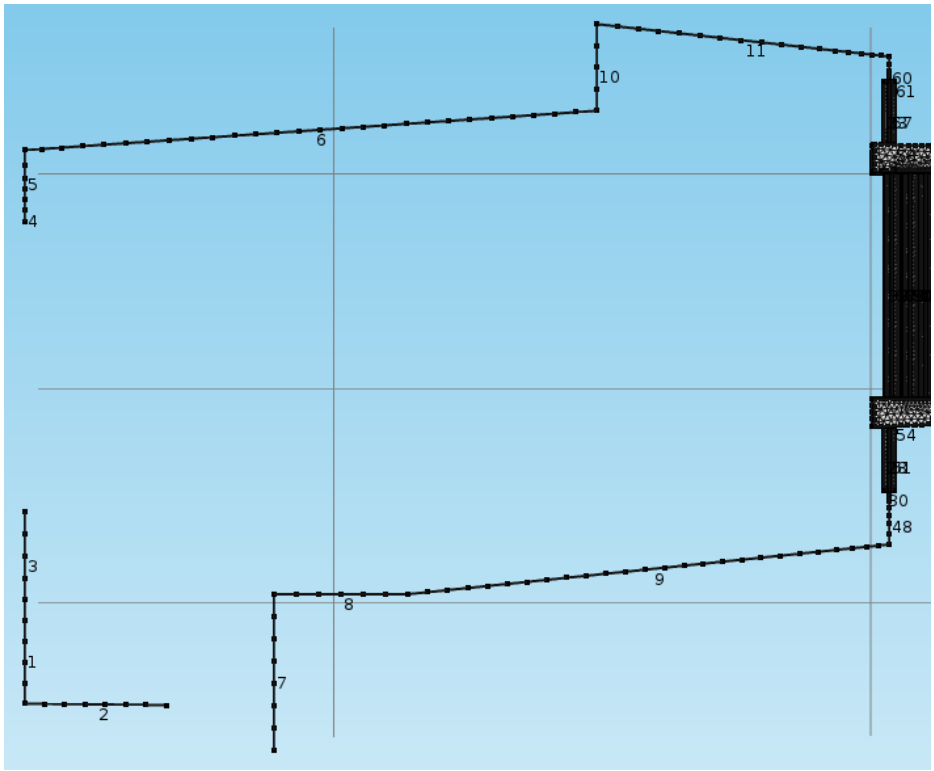

Figure 10. Piping Mesh.

4.3.3 Heat Exchanger. The LSTL heat exchanger was meshed using COMSOL's default 'Fine' setting for fluid dynamics. 4 boundary layer nodes were added to the mesh to capture the near-wall flow characteristics. The first layer thickness adjustment factor was set to 0.5 to ensure the first boundary layer nodes were located in

the viscous sublayer. This mesh consisted of 332,912 elements and accounted for a vast majority of the size of the model. Fluid velocity in the heat exchanger inlet and outlet, as well 13 of 14 heat exchanger tubes was found to be turbulent. So in addition, running a k-epsilon turbulence model on this fine mesh accounts for nearly all of the degrees of freedom in the model. This mesh size was selected for convergence and run-time. The model with the current mesh, shown in Figure 11, takes about 6.5 hours to solve and has an average velocity inlet/outlet difference of only 2.3%. The mesh is shown below.

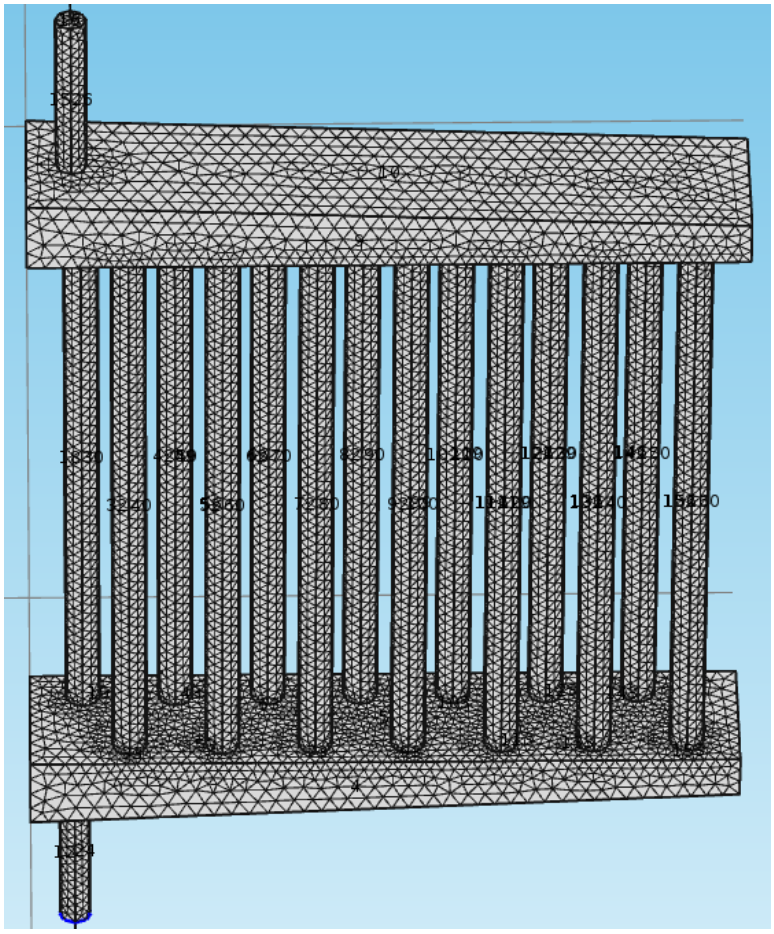

Figure 11. Heat exchanger mesh.

Because the heat exchanger tube walls are only 0.065” thick, the mesh also needed to be fine enough to accurately represent the geometry of the inner and outer tube diameters. The next mesh size down squares off significant parts of the tubes and does not accurately calculate conduction through the tube wall to the outer heat transfer coefficient. A blown-up view of the mesh at the inner and outer tube walls is shown below in Figure 12.

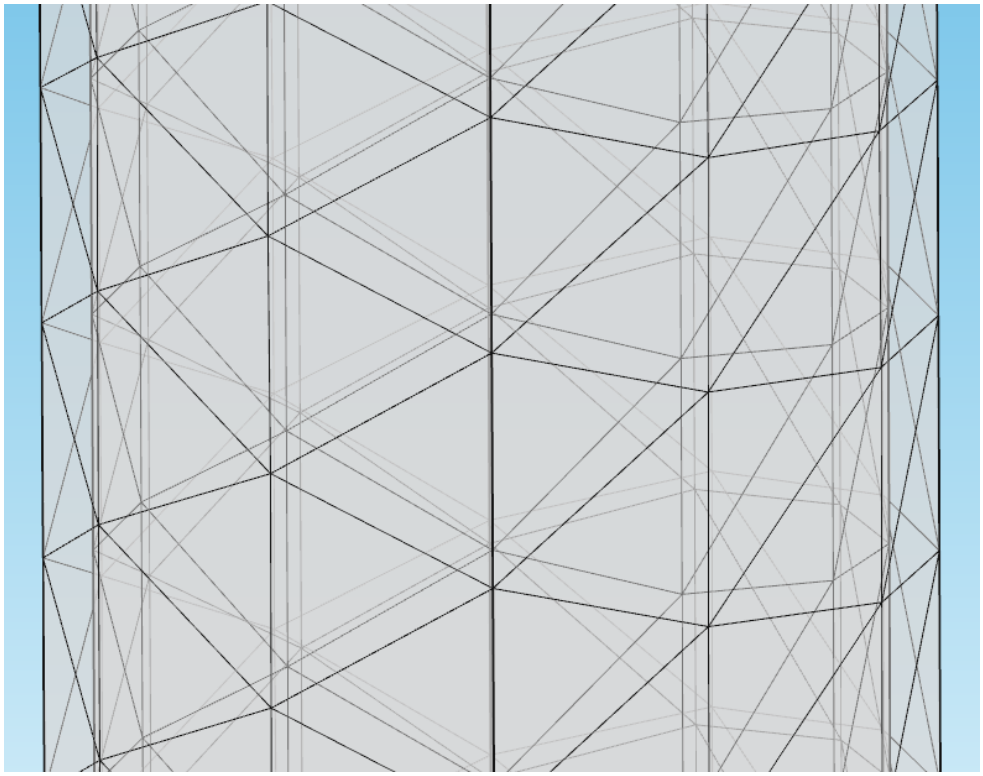

Figure 12. Blown-up view of the heat exchanger mesh in the tube walls.

4.4 Model Couplings and Issues

4.4.1 Coupling Separate Models. COMSOL is designed so that the user can develop and solve multiple models within a single COMSOL file. This allows models

made in different spatial geometries (1D, 2D, 3D) to be coupled together and solved simultaneously. The variable coupling used in this model is performed by using average and integration operators. Variable coupling is performed at 1D points, and 2D and 3D boundaries. In order to couple variables at a 1D point to a 3D boundary, the integration operator is used. Because the variable at the 1D point is a scalar value, the integration operator applies the scalar value to the entire 3D boundary. In order to couple variables at a 3D boundary to a 1D point, the average operator is used. The average operator averages the variable across the 3D boundary and applies that scalar value to the 1D point. These coupling operators are used to couple pressure, velocity, and temperature at each of the 1D-3D and 1D-2D interfaces. Loop inlet and outlet temperature are not coupled, resulting in an open loop simulation.

A major benefit of the 1D Pipe Flow module is that the 1D calculation can be performed on lines in a 3D geometry. This allows the user to model both 1D and 3D components in the same 3D geometry. So for the LSTL model, all 1D pipe flow and 3D turbulent flow sections are built in the same model. However, the pebble bed section must be built in a separate model because the porous media physics are calculated in a 2D-axisymmetric geometry. The pebble bed inlet velocity is dependent upon the outlet velocity of the upstream pipe section, and the pebble bed outlet pressure is dependent upon the downstream pipe pressure. Inlet and outlet pebble bed temperatures are transferred to the pipe section temperatures at the interfaces.

If both of the coupling variables at an interface are in the same model, then only the basic operator syntax is required to call the coupling operator. Basic coupling operator syntax is shown below:

Integration = intop#(variable)
Average = aveop#(variable)

The # sign indicates which integration or average operator is to be called, and the 'variable' indicates the required COMSOL syntax for whichever variable the operator will evaluate. For example, to average the velocity at a 3D boundary, an average operator is assigned to that boundary: aveop1. The COMSOL syntax for fluid velocity is spf.U, so the full operator syntax is aveop1(spf.U). In the same manner, to integrate the pressure at a 1D Pipe Flow point, the full operator syntax would be intop1(p) where p is the pipe flow pressure.

4.4.2 Coupling Variables. If the coupling variables at an interface are not located in the same model, then global variables must be used. This occurs at the pebble bed inlet and outlet, where 1D pipe flow variables are called from the 3D model to the 2D-axisymmetric porous media model. To add global variables to the model, a variables node must be added to the model under global definitions (shown in Figure 13). Any variables listed under global definitions are available in all of the models built within the COMSOL file.

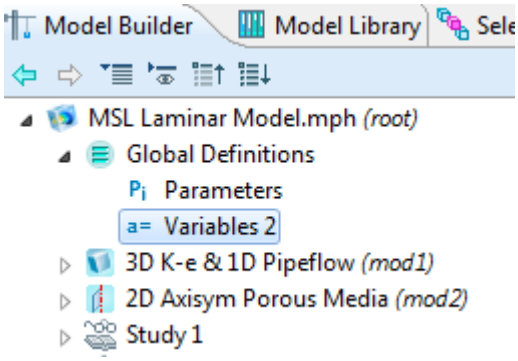

Figure 13. Global variables shown in the COMSOL GUI.

4.5 Various Errors

It is important to note that although the coupling worked well, getting past various errors and model setup issues took a considerable amount of time. One particular Navier-Stokes error was never fully understood even when COMSOL was contacted about the issue. This Navier-Stokes error would typically come up when trying to create different meshes in an effort to perform a mesh refinement study. This issue led to certain mesh and boundary layer combinations resulting in errors for unexplained reasons.

Another issue that took some time to work through was setting the coupled variables to apply reaction terms on ‘individual dependent variables’. The reaction term is a term used by COMSOL to represent the constraints placed on variables at a boundary condition. The default setting is to apply reaction terms on ‘all physics (symmetric)’. Under the default setting, reaction term forces are generated at the boundary for the zero Neumann constraint. However, in this case, because a non-zero quantity is being coupled between the 1D and multidimensional boundaries, the Neumann constraint does not hold and a reaction term must be computed to perform the coupling. The model couplings will

not work and the simulation will fail until these constraint settings are changed to apply reaction terms on ‘individual dependent variables’.

It was also discovered that model convergence was limited by the mesh size in the 2D-axisymmetric porous media section. The segregated step containing the pebble bed variables would flat-line at a value above convergence (0.02, for example). This is still not fully understood, as the porous media section solves quickly with fine meshes when run separately from the rest of the model. In order to attain convergence of the coupled model, the porous media section uses COMSOL’s default ‘coarser’ mesh setting. 5 boundary layer nodes were added to capture the high voidage areas that occur near the wall in the pebble bed. By studying this section independently from the rest of the loop, it was discovered that a finer mesh did not have a significant impact on results.

4.6 Computing Power

A Dell Precision T3500 workstation was used to run COMSOL. This desktop was equipped with an Intel Xeon quad-core CPU rated at 2.80 Ghz, with 24 GB of RAM. A segregated, 3 group solver was used to compute the coupled model. Direct solvers were used with each segregated step. Convergence criteria for all 3 solvers was set to 0.001.

Chapter 5 Porosity Profile Comparison

In the graphite pebble bed, there is an average radial voidage variation due to the effect of the SiC wall. Theoretically, the voidage will be greatest at the wall where the pebble packing is at a minimum. Moving away from the wall, the voidage will vary radially due to random packing until it reaches a steady average value at a certain distance from the wall. However, because the pebble bed in the LSTL is only 5 pebble diameters wide, the average voidage never reaches an unchanging spatial average across the pebble bed. Establishing the correct porosity profile in the COMSOL model is important to accurately model the pressure drop and temperature increase through the pebble bed. In the porous media module, COMSOL requires porosity and permeability inputs. These values were input to COMSOL using tabulated data with an interpolation function.

Tabulated radial voidage data was produced for the graphite pebble bed by Dr. Gary Mueller at Missouri University of Science & Technology. Dr. Mueller has designed a widely recognized code that generates porosity profiles for pebble beds of various dimensions (Ref. 12 & 13). His code requires pebble diameter, bed diameter, and bed length to develop an average radial porosity profile. Dr. Mueller's code-generated porosity profile for the LSTL is shown below in Figure 14. The data shows a uniform porosity profile out to 1 sphere diameter, at which point the packed bed randomization begins to impact the profile. Notice that the second porosity peak is at slightly less than 2 sphere diameters from the wall. This is due to pebbles randomly overlapping, where the outer edge of the next pebble is inside of 1 sphere diameter from the wall. The extreme

low porosity value on the profile is due to the wall effect causing an axial centerline column of pebbles. The first pebble layer, shown below in Figure 13, shows an outer wall ring of pebbles, an inner ring, and a single centerline pebble. The D/d value referenced is the ratio of bed diameter to pebble diameter.

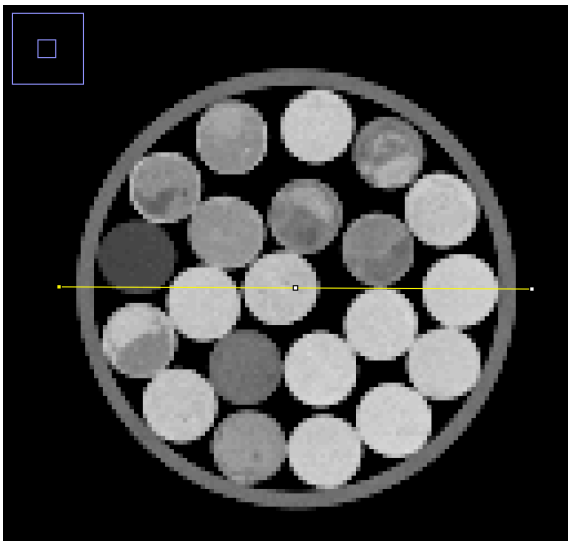

Figure 13. CT scan of first layer pebbles at ½ sphere diameter from the bottom plate.

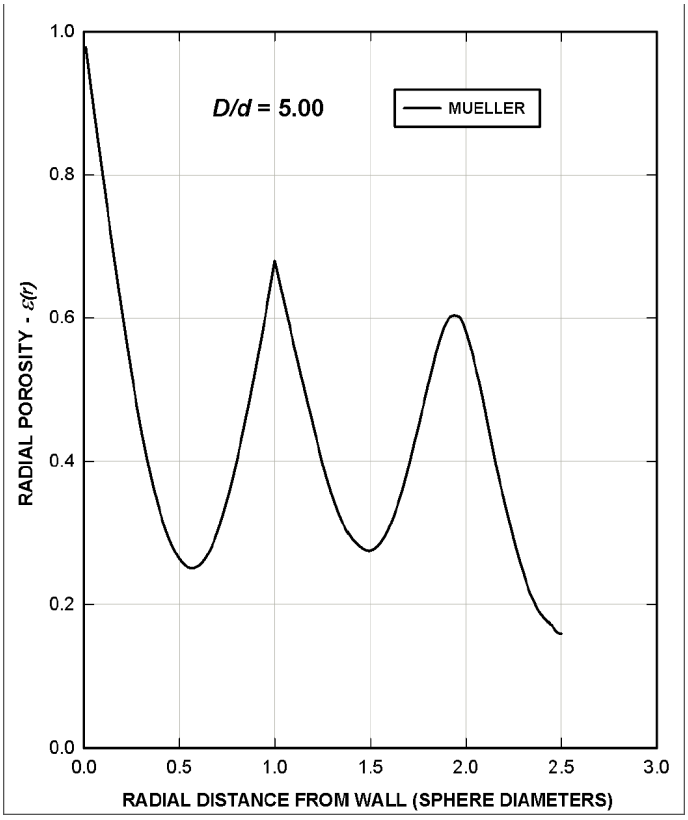

Figure 14. Average radial porosity profile generated by Mueller.

The University of Tennessee Department of Nuclear Engineering has a partnership with UT Medical Center to use medical equipment for research purposes. In order to validate the results of Dr. Mueller's code, a modular pebble bed was CT-scanned and the density profiles were compared. The pebble bed was a 17" long acrylic cylinder with a 5.5" ID filled with 1" diameter rubber balls. In order to reduce x-ray scatter and maintain the integrity of the scan, the amount of metal objects in the scanner needed to be minimized. The bottom of the modular pebble bed is supported by a metal screen that is needed to support the pebbles. For the CT scan, a polyethylene circular plate was inserted

between the rubber spheres and metal screen to reduce the effect of x-ray scatter from the metal screen. The modular pebble bed is shown below in Figure 15.

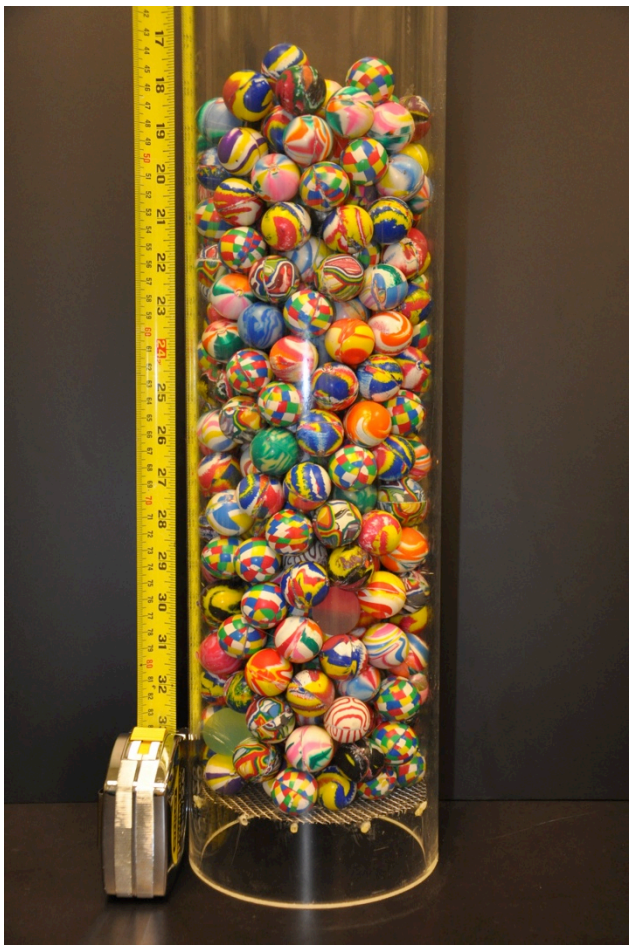

Figure 15. Modular Pebble Bed.

The software used with the CT scanner at UT Medical Center produces a DICOM file for every slice taken during the scan. In order to view the DICOM files correctly, an open source software program called Image J was used. Image J allows the user to import a sequence of DICOM file images and view the data slice by slice. Figure 16 shows a

radial slice and its corresponding density profile. In order to develop an average porosity profile from the DICOM files, over 100 slices were taken from the data and imported to Excel. Gray values were then converted to porosity values by using a calibration curve. It was determined from the data that a gray value of -1000 corresponded to a porosity of 1, and a gray value of 750 corresponded to a porosity of 0. This resulted in a calibration curve of

$$\varepsilon = -0.000571 \times GV + 0.42825$$

where GV = gray value.

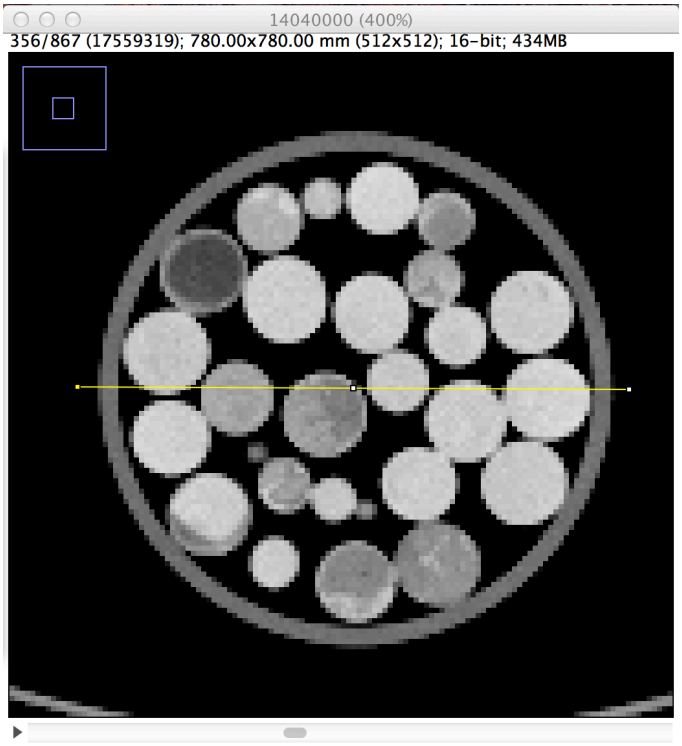

Figure 16. View of a single radial slice.

Figure 17. Density profile for a single radial slice along the yellow line in Figure 16.

Once the calibration curve was applied to the data in Excel, the porosity was averaged for all of the slices, and a single average radial profile was generated, shown below in Figure 18.

Because the modular pebble bed has dimensions that differ slightly from the pebble bed in the LSTL, the CT scan results were compared to code-generated results from Dr. Gary Mueller at Missouri University of Science & Technology. It was determined that the CT-scan generated porosity profile matches D/d= 5.96. D/d for the representative pebble bed is 5.5. The porosity profile used in the COMSOL model is one generated from Dr. Mueller's code with D/d = 5, which matches the LSTL pebble bed geometry.

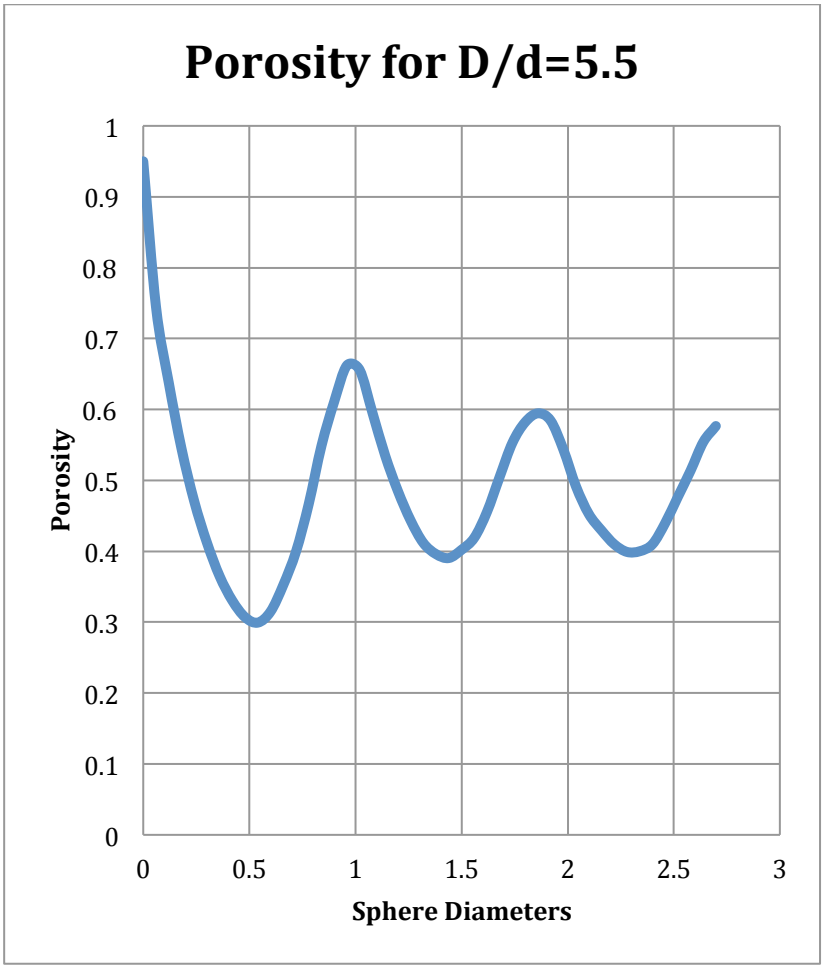

Figure 18. CT-scan generated porosity profile.

Chapter 6 COMSOL Results

6.1 Salt Loop

Results of the multidimensional coupled LSTL model are presented in the following figures. The pressure distribution through the LSTL shows most of the pressure drop occurs through the 1” pipe sections before and after the heat exchanger, as expected. The LSTL total pressure drop was found to be 203,398 Pa. LSTL pressure distribution is shown in Figure 19. Minor losses in the heat exchanger are calculated by COMSOL. The pebble bed section of the LSTL was built in a different modeling dimension (2D-axisymmetric), so the results for the pebble bed cannot be shown in the same window as the rest of the LSTL. Pebble bed results are presented separately.

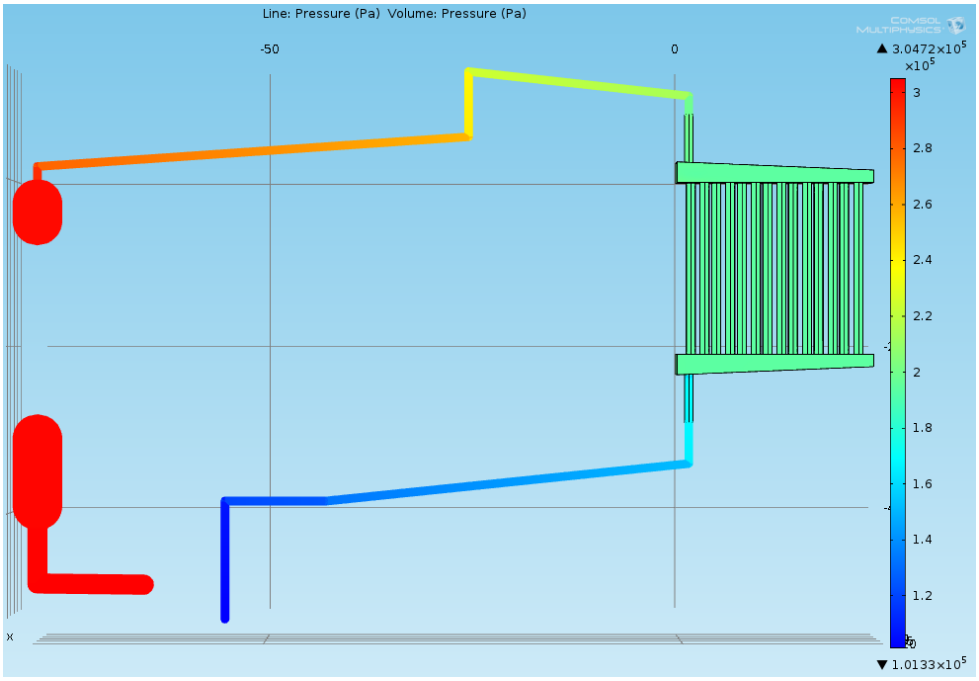

Figure 19. LSTL Pressure.

The velocity distribution in the LSTL shows good agreement before and after the pebble bed, and before and after the heat exchanger. LSTL velocity distribution is shown in Figure 20. The average fluid velocity is 3.96 m/s at the heat exchanger inlet, and 3.87 m/s at the heat exchanger outlet. This is a difference of 2.3%. At the pebble bed inlet and outlet, the fluid velocity is 0.126 m/s and 0.121 m/s, respectively. This is a difference of 3.9%.

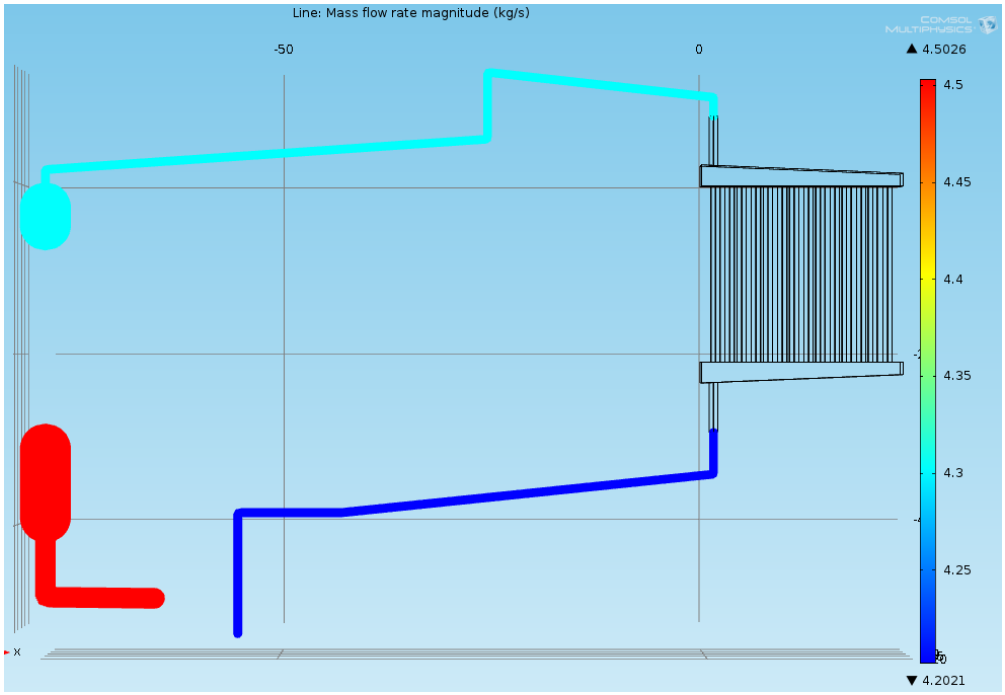

Figure 20. Mass flow in the LSTL piping sections.

The LSTL temperature distribution shows an interesting low-flow section in one of the heat exchanger tubes. This phenomena is presented further in the heat exchanger results. The LSTL model results show an overall loop ΔT of -8.6 °C, indicating more heat is rejected by the air-cooled heat exchanger than is put into the system with loop induction heating.

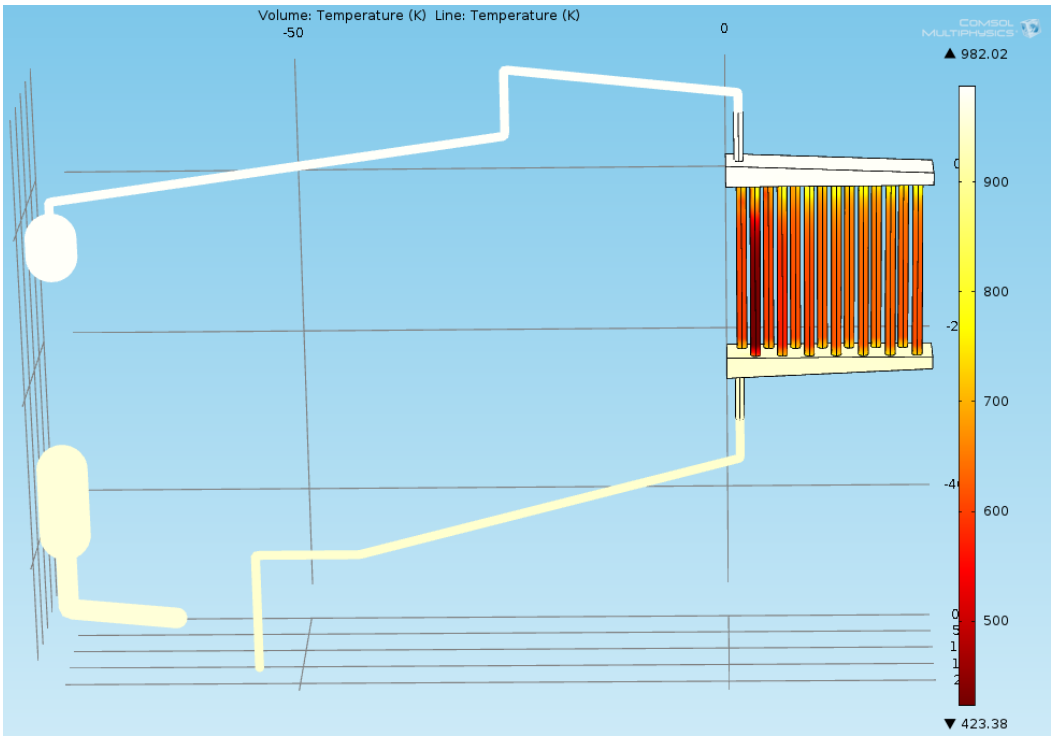

Figure 21. LSTL Temperature.

6.2 Pebble Bed

The pebble bed velocity distribution largely follows the porosity profile. In the near-wall region where voidage is highest, the fluid velocity is highest. Fluid velocity is at a minimum at the pebble bed centerline where porosity is also at a minimum. The max fluid velocity is 0.5 m/s near the SiC wall, while most of the pebble bed exhibits a fluid velocity between 0 and 0.2 m/s. Viscous losses in the pebble bed result in a ΔP of 1137 Pa.

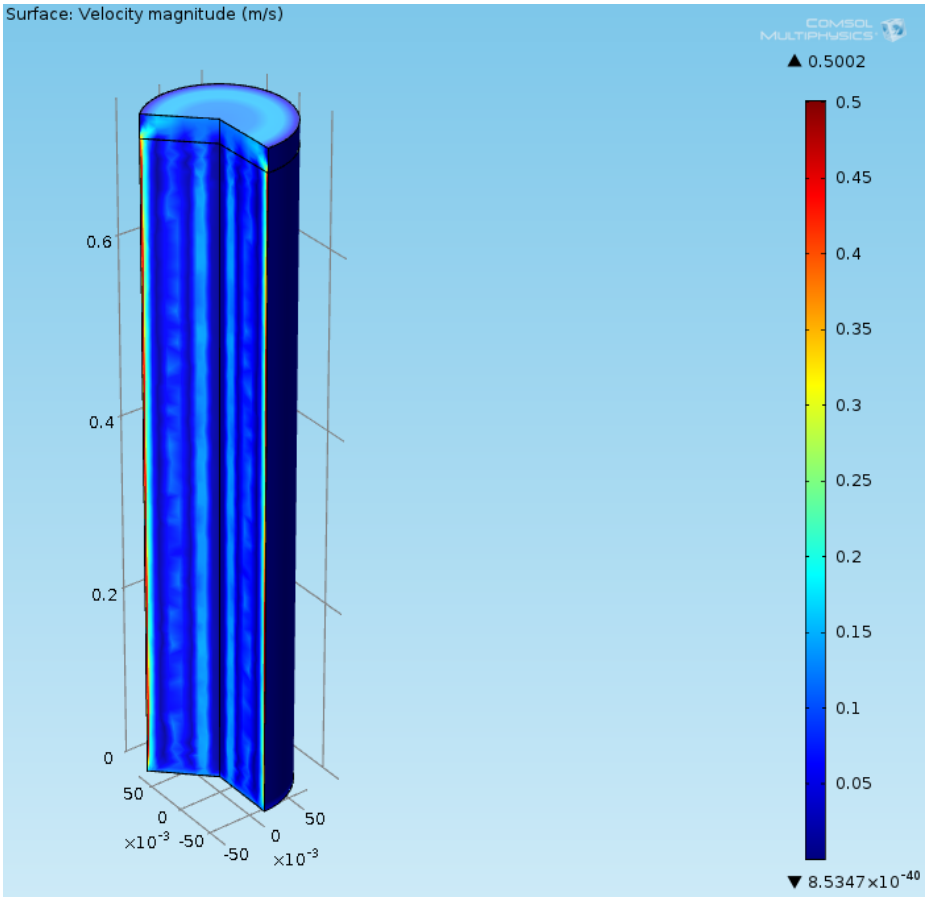

Figure 22. Pebble bed velocity.

The pebble bed temperature distribution largely follows the velocity distribution, as expected. The pebble bed average outlet temperature is higher than a hand calculation energy balance predicts at 708.7 °C. The LSTL inlet temperature is set at 680 °C, resulting in a pebble bed ΔT of 28.7 °C. This ΔT is higher than expected due to COMSOL performing an area average at the pebble bed outlet. A mass flow averaged outlet temperature, which is unavailable in COMSOL, would result in a more accurate ΔT. Inlet temperature to the 1" piping section above the pebble bed is set by the model coupling, based on the average pebble bed outlet temperature.

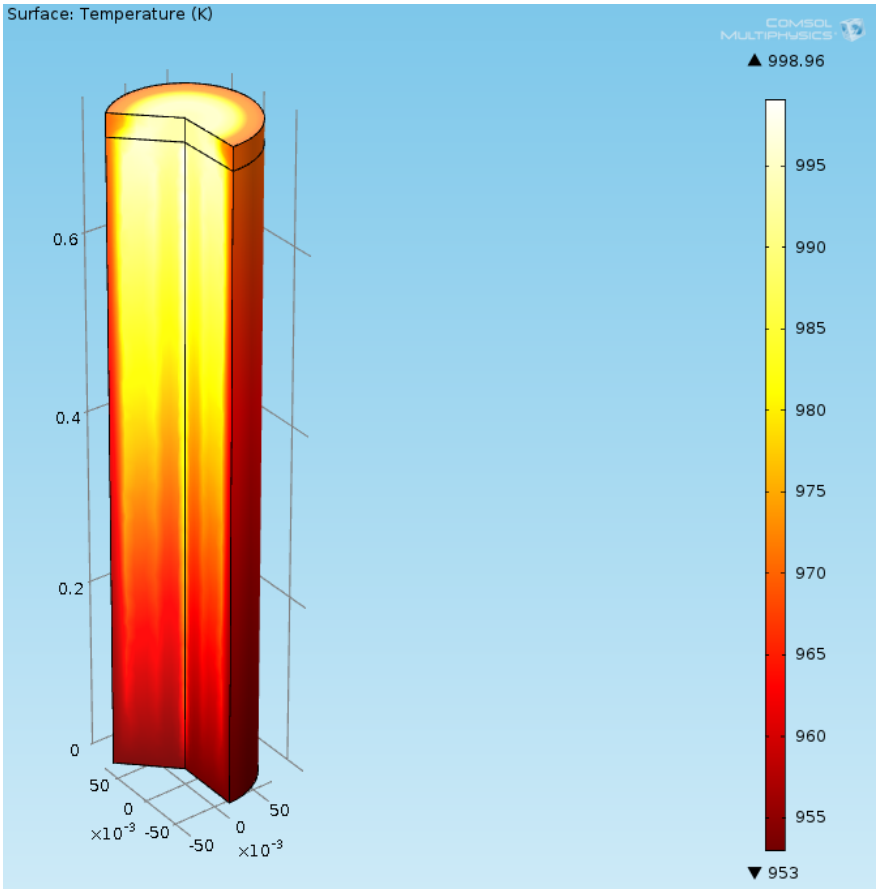

Figure 23. Pebble bed temperature.

6.3 Heat Exchanger

The heat exchanger exhibits a larger than expected ΔT of 37.3 °C. This larger ΔT is due to the heat transfer coefficient being calculated with a high air coolant velocity. As a safety precaution, the heat exchanger is designed to remove more energy than can be put into the system. During loop operation, the air velocity will have to be adjusted in order to establish a steady state where the heat exchanger ΔT matches the pebble bed ΔT. Temperature distribution in the heat exchanger is shown in Figure 24.

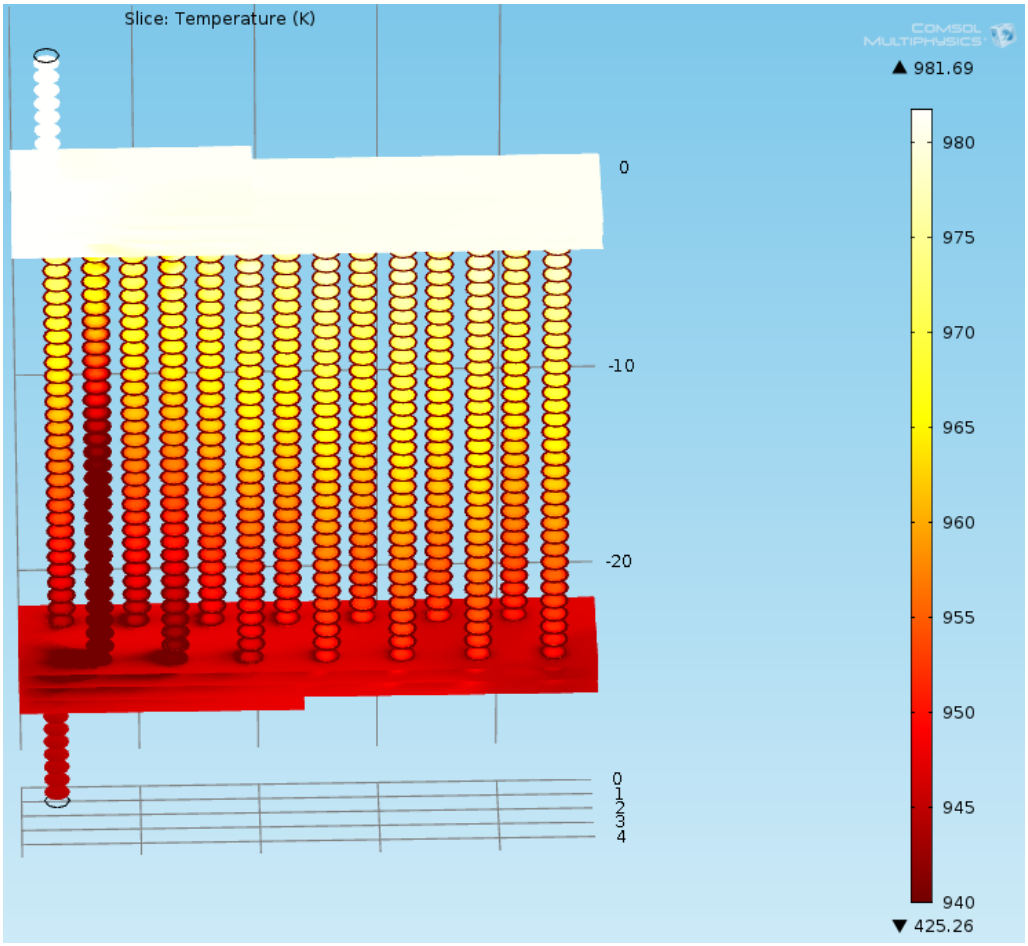

Figure 24. Heat exchanger temperature distribution.

Wall lift-off (y+) values were generated for the mesh used in the heat exchanger. y+ values of 11.06 are achieved in all of the heat exchanger tubes. COMSOL recommends that y+ = 11.06 in all 3D fluid flow sections to ensure that all boundary layer nodes are located in the viscous sublayer (Ref. 5). y+ = 11.06 is the distance from the wall where the logarithmic layer meets the viscous sublayer. y+ values greater than 11.06 are found only at the sudden expansion located in the upper plenum of the heat exchanger. y+ values greater than 11.06 indicate the first boundary layer mesh cells near the wall are located further up in the logarithmic layer. y+ values are shown for the heat exchanger in Figure 25.

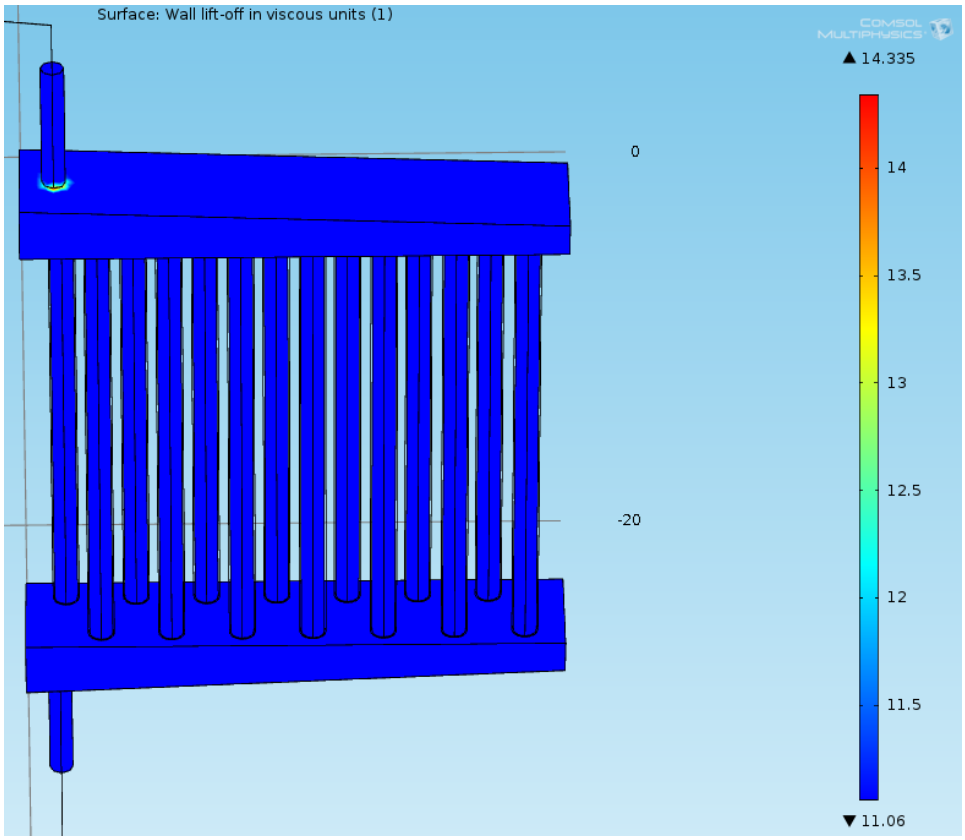

Figure 25. Heat exchanger y+ values.

The heat exchanger flow distribution indicates that one tube (2nd from the left) has a significantly smaller flow velocity than any of the other tubes. This tube has a velocity of less than 0.1 m/s. Most tubes have a velocity between 0.2 and 0.35 m/s. The heat exchanger flow distribution is shown in Figure 26. In the future, examining the kinetic energy and pressure distribution in the heat exchanger header would be valuable in assessing the cause of this mal-distribution.

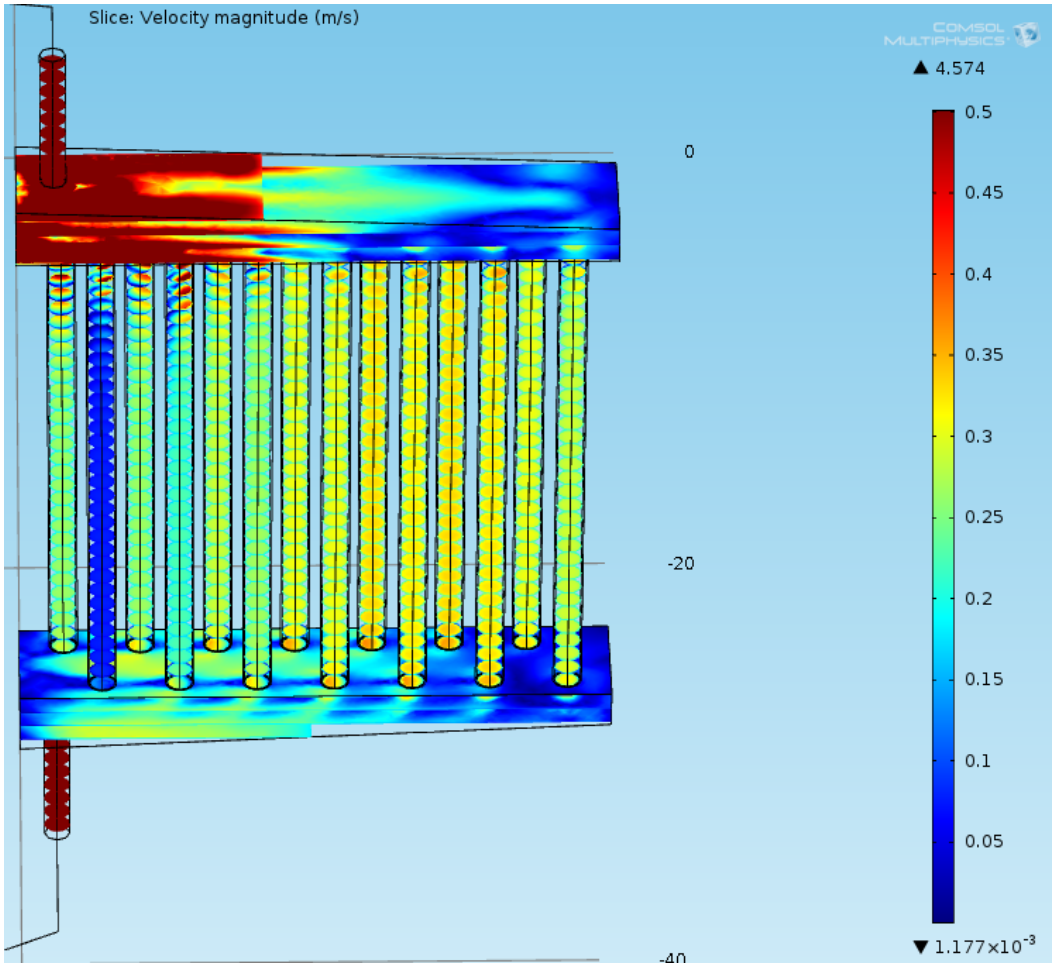

Figure 26. Heat exchanger velocity showing flow distribution in tubes.

Table 2. LSTL Model Results

Component	***ΔP, Pa***	***ΔT, °C***
Pebble Bed	1137	+28.7
Heat Exchanger	30,784	-37.3
LSTL	203,398	-8.6

The COMSOL pressure results show good agreement with the expected results from Ref. 3. Both the AFT Fathom model and the Bernoulli loop analysis presented in the following sections generate pressure drops lower than COMSOL or Ref. 3. Coolant temperature rise in the pebble bed and temperature decrease in the heat exchanger both differ from results in Ref. 3. In addition to reasons previously discussed, being able to perform a mesh refinement analysis would be valuable in assessing the accuracy of these results.

6.4 Verification

6.4.1 AFT Fathom. In order to verify pressure and velocity results from the coupled model generated in COMSOL, a much simpler model of the LSTL was built in AFT Fathom. AFT Fathom is an incompressible pipe flow analysis and system modeling software for engineers used to calculate pressure drop, flow velocity, and flow distribution. The AFT Fathom model is shown in Figure 27.

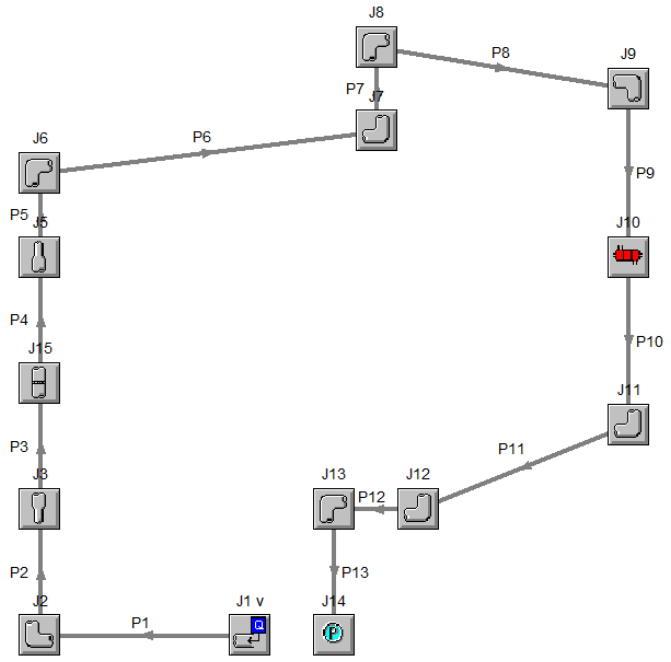

Figure 27. AFT Fathom model of the LSTL.

An assigned mass inflow of 4.5 Kg/s acted as the pump for the system. Pipe sections with defined diameters and elevations set to the LSTL parameters make up most of the model. The pebble bed is represented by a general component with a circular wire screen that cuts down the flow area to one half of the bed diameter. This yields a pressure drop (2.07 psi) similar to that of the pebble bed as calculated by the Ergun equation (2.16 psi). The heat exchanger was selected in the AFT Fathom GUI as a single pass heat exchanger with a 21-inch long, 14-tube configuration. Minor losses at bends, contractions, and expansions were calculated by AFT Fathom. Pressure at the loop outlet was set to be atmospheric.

AFT Fathom solves input models by performing 1D incompressible hydraulic calculations using Newton-Rapshon matrix methods. This allows the code to solve very quickly, with this model converging in only 2 iterations and requiring only 0.05 seconds. Tabulated results data is presented below in Tables 3 and 4. Total pressure drop through the loop is 20.8 psig (143,371 Pa) at the assigned mass flow rate of 4.5 Kg/s.

Table 3. Results of the LSTL model built in AFT Fathom for pipe sections.

Pipes

Pipe	Name	Velocity (meters/sec)	P Static In (psig)	P Static Out (psig)
1	Pipe	0.7620	20.8357	2.082E+01
2	Pipe	0.7620	20.8031	2.011E+01
3	Pipe	0.1261	20.1575	1.957E+01
4	Pipe	0.1261	17.5045	1.732E+01
5	Pipe	3.9953	13.8446	1.330E+01
6	Pipe	3.9953	12.5545	9.714E+00
7	Pipe	3.9953	8.9673	8.001E+00
8	Pipe	3.9953	7.2544	6.177E+00
9	Pipe	3.9953	5.4309	5.645E+00
10	Pipe	3.9953	4.0040	4.281E+00
11	Pipe	3.9953	3.5342	1.507E+00
12	Pipe	3.9953	1.0995	5.257E-01
13	Pipe	3.9953	-0.2209	9.537E-07

Table 4. Results of the LSTL model built in AFT Fathom for all components.

All Junctions | Area Change | Assigned Flow | Assigned Pressure | Bend | Heat E

Jct	Name	P Static In (psig)	P Static Out (psig)	Mass Flow Rate Thru Jct (kg/sec)	Loss Factor (K)
1	Assigned Flow	2.084E+01	2.084E+01	4.500	0.0000
2	Bend	2.082E+01	2.080E+01	4.500	0.2547
3	Area Change	2.011E+01	2.016E+01	4.500	0.4074
5	Area Change	1.732E+01	1.384E+01	4.500	490.2927
6	Bend	1.330E+01	1.255E+01	4.500	0.3193
7	Bend	9.714E+00	8.967E+00	4.500	0.3193
8	Bend	8.001E+00	7.254E+00	4.500	0.3193
9	Bend	6.177E+00	5.431E+00	4.500	0.3193
10	Heat Exchanger	5.645E+00	4.004E+00	4.500	1.5131
11	Bend	4.281E+00	3.534E+00	4.500	0.3193
12	Bend	1.507E+00	1.100E+00	4.500	0.1742
13	Bend	5.257E-01	-2.209E-01	4.500	0.3193
14	Assigned Pressure	9.537E-07	9.537E-07	4.500	0.0000
15	Screen	1.957E+01	1.750E+01	4.500	1.6499

6.5 Hand Calculations

6.5.1 Ergun Equation- Pressure Drop in Pebble Bed. Pressure drop in randomly packed beds can be hand calculated using the standard 1D viscous loss model with a fanning friction factor, which is based on the void fraction in a packed bed volume. The fanning friction factor for turbulent flows is defined

$$f_f = \frac{f}{4} = 0.875\left[\frac{1-\varepsilon}{\varepsilon^3}\right]$$

where

f = darcy friction factor
ε = void fraction

In order to use the fanning friction factor for fully turbulent flows, the following equation must be satisfied:

$$\frac{\left[\frac{\rho v_o D_{fuel}}{\mu}\right]}{1-\varepsilon} > 1000$$

where

ρ = fluid density
v_o = superficial bed velocity
D_{fuel} = pebble fuel diameter
μ = fluid viscosity

At a mass flow rate of 4.5 Kg/s, with ρ = 2020 Kg/m^3, D_{fuel} = 0.03 m, and

μ = 0.0029 Pa-s, the turbulence equation $\frac{\left[\frac{\rho v_o D_{fuel}}{\mu}\right]}{1-\varepsilon} = 5{,}269$ which confirms that the flow in the LSTL pebble bed is fully turbulent. Assuming the LSTL pebble bed porosity, ε = 0.5, the fanning friction factor is 3.5. Now the friction factor can be applied to the standard 1D viscous loss model:

$$P_1 - P_2 = \tfrac{1}{2}\rho v^2 \left(4 f_f \tfrac{L}{D}\right)$$

where

L = bed length
D = bed diameter

For the LSTL pebble bed, L = 0.7 m and D = 0.15 m. This results in a viscous loss of 1,048 Pa. This pressure drop agrees very well with the 2.07 psig (14,268 Pa) pressure drop calculated in AFT Fathom.

6.5.2 Bernoulli for LSTL. In order to hand calculate the pressure loss throughout the rest of the loop, an analysis was performed using Bernoulli's incompressible flow equation, shown below:.

$$\frac{P_1}{\rho g} + \frac{V_1^2}{2g} + z_1 = \frac{P_2}{\rho g} + \frac{V_2^2}{2g} + z_2 + h_L$$

Pressure drop through the heat exchanger was assumed to be 1.64 psig (11,304 Pa), as calculated by AFT Fathom. The Bernoulli analysis with appropriate minor losses for bends, elbows, expansions, etc. yields a total LSTL pressure drop of 23.8 psig (164,050 Pa) at the operating flow rate of 4.5 Kg/s.

6.6 Comparison of Results

Results from the COMSOL LSTL model, AFT Fathom model, hand calculations, and references are presented in Table 5.

Table 5. Results Comparison

Simulation	***ΔP, Pa***	***ΔT Pebble Bed, °C***	***ΔT Heat Exchanger, °C***
COMSOL	203,398	28.7	37.3
Ref. 3	205,407	20	20
AFT Fathom	143,371	-	-
Hand Calculation	164,050	23.6	-

For this model, main experimental data points of interest are ΔP_{pump}, $\Delta T_{pebble\ bed}$, and $\Delta T_{heat\ exchanger}$. Table 5 indicates that ΔP_{pump} predicted by COMSOL agrees well with Ref. 3. $\Delta T_{pebble\ bed}$ predicted by COMSOL is higher than Ref. 3 or an energy balance calculation. This discrepancy is likely due to average couplings being dependent on geometry instead of mass flow. $\Delta T_{heat\ exchanger}$ predicted by COMSOL is higher than Ref. 3. This discrepancy is likely due to the volumetric flow of air used in the Nusselt correlation being set to the loop design rate, which is meant to remove more heat from the system than can be added by the pebble bed. It is important to recognize that Ref. 3 results are for a closed loop, and the LSTL COMSOL model is an open loop simulation. The open loop simulation, with a defined loop inlet temperature of 680 °C, allows the energy input to the system to differ from energy removed by the system. During LSTL

operation, air flow over the heat exchanger will have to be varied with fan speed so $\Delta T_{heat\ exchanger}$ matches $\Delta T_{pebble\ bed}$.

Future work on the LSTL model could involve closing the loop by coupling the inlet and outlet temperature. This would allow the loop temperature to vary until heat sink performance matches the energy input to the system. In addition, examining the kinetic energy and pressure distribution in the heat exchanger header would be valuable in assessing the cause of heat exchanger mal-distribution.

Chapter 7 Conclusions and Recommendations

The LSTL model designed in COMSOL provides a computationally efficient simulation tool that determines temperature, pressure, and velocity at any point in the loop. Working with COMSOL in a multidimensional manner requires advanced knowledge of COMSOL's default code settings and the necessary changes required to make couplings possible. This takes away from COMSOL's practicality as an easy-to-use modeling tool, but its multidimensional functionality is one of a kind in the current CFD arena. The LSTL model developed is unique in its use of 1D, 2D, and 3D fluid flow and heat transfer sections. Ultimately, COMSOL's multidimensional modeling capability allows it to be a valuable resource for modeling large fluid flow and heat transfer systems in an efficient and accurate manner.

The integrated LSTL model presented herein is validated against a 1D AFT Fathom pipe network model, and component models are tested against established engineering models via hand calculations. In general, agreement is good, and a high degree of confidence is established in the fidelity of the COMSOL simulation.

The integrated model predicts temperatures and pressures at measurement locations in the LSTL. This will allow refinement of models going forward, and may inform design improvements for the loop and salt cooled pebble bed reactor. The loop data may also be formally used as validation, following ASME Standard V V 20.

List of References

1. C. L. Barnard, et. al., "A Theory of Fluid Flow in Compliant Tubes," *Biophysical Journal,* Volume 6**,** *no. 6,* 717-724 (1966).

2. D. F. Williams, *Assessment of Candidate Molten Salt Coolants for the NGNP/NHI Heat-Transfer Loop.* ORNL/TM-2006/69, Oak Ridge National Laboratory, Oak Ridge, TN.

3. G. L. Yoder Jr, et al. *High Temperature Fluoride Salt Test Loop.* ORNL/TM-2012/430, Oak Ridge National Laboratory, Oak Ridge, TN.

4. N. E. Todreas and M. S. Kazimi, *Nuclear Systems: Thermal Hydraulic Fundamentals*, Vol. 1, CRC Press, Boca Raton, FL (2012).

5. COMSOL Multiphysics. "CFD Module User's Guide." *COMSOL Multiphysics User's Guide.* Boston: COMSOL Multiphysics, May 2013.

6. COMSOL Multiphysics. "Pipe Flow Module User's Guide." *COMSOL 4.3b User's Guide.* Boston: COMSOL Multiphysics, May 2013.

7. University of California - Berkeley. *Pebble Bed Advanced High Temperature Reactor.* http://pb-ahtr.nuc.berkeley.edu/index.html (accessed August 29, 2013)

8. R. B. Bird, W. E. Stewart, and E. N. Lightfoot, *Transport Phenomena,* 2nd Ed., 188-192, Wiley, New York (2007)

9. S. Kakac, et al, *Heat Exchangers Thermal Hydraulic Fundamentals and Design,* Hemisphere Publishing Corporation, Washington DC (1981)

10. S. Kakac, et al, *Handbook of Single-Phase Convective Heat Transfer*, Wiley & Sons, New York (1987)

11. C. W. Forsberg, P. F. Peterson, H. Zhao, *An Advanced Molten Salt Reactor Using High-Temperature Reactor Technology.* Paper 4152, 2004 International Congress on Advances in Nuclear Power Plants, Pittsburgh, PA.

12. G. E. Mueller, *Numerically Packing Spheres in Cylinders*. Powder Technology, 159, 105-110 (2005)

13. G. E. Mueller, *Radial Porosity in Packed Beds of Spheres.* Powder Technology, 203, 626-633 (2010)

14. S. B. Pope, *Turbulent Flows.* Cambridge University Press, Cambridge (2003)

Appendix

Tables for Pressure Loss and Hand Calculations

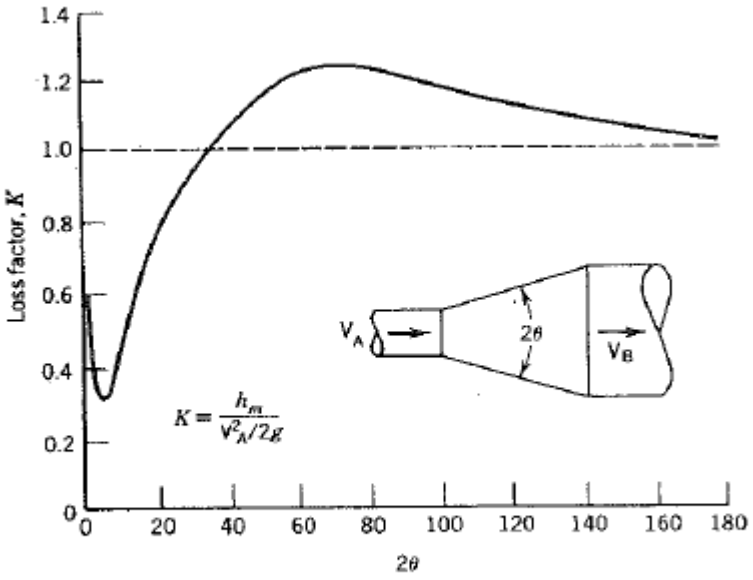

Figure 7-8 Loss factor K for a gradual conical expansion.

Figure A1. Loss factor K for a gradual conical expansion.

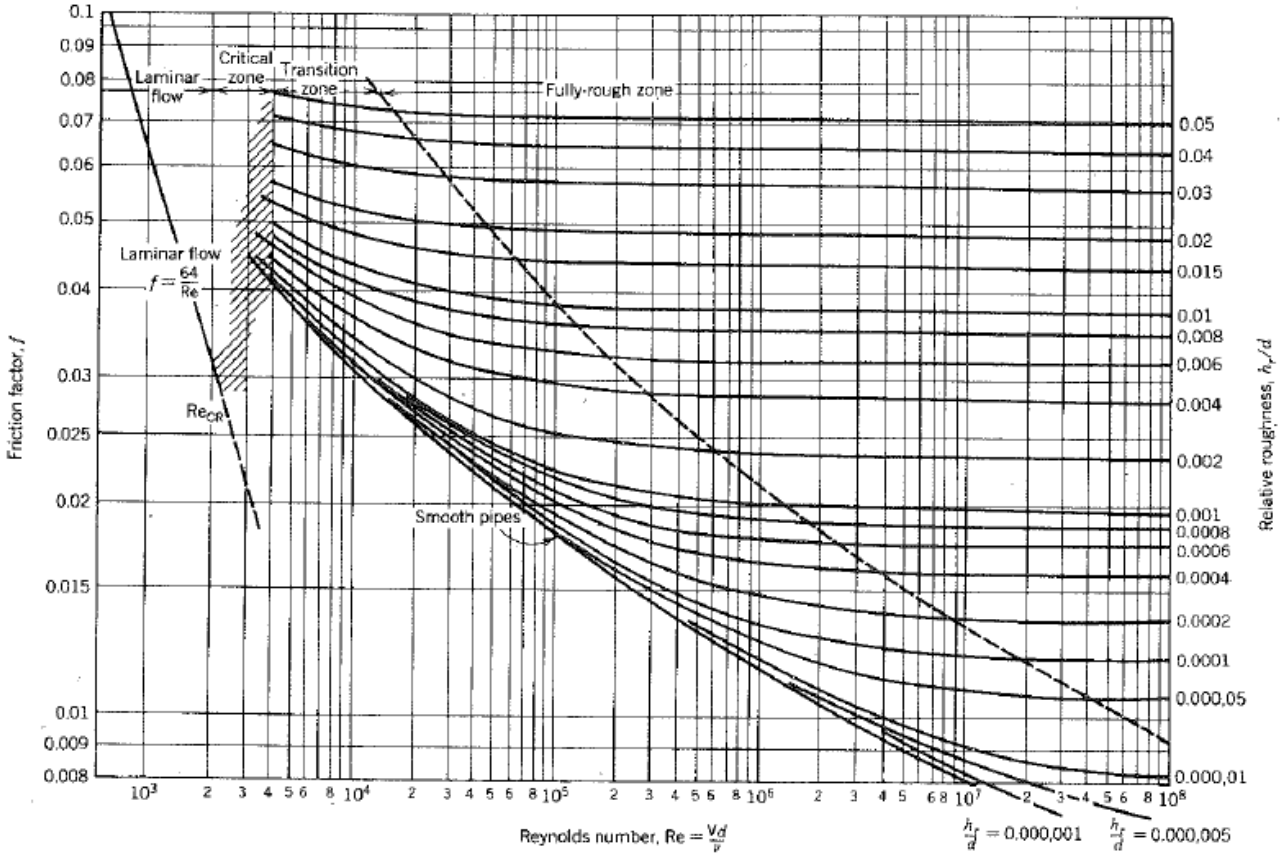

Figure 7-4 Friction factor for fully developed circular duct flows.[2] Used with permission.

Figure A2. Friction factor for fully developed pipe flows.

Table 7-2 Loss Factor, $K = \frac{h_m}{V_A^2/2g}$ for Open Valves, Elbows, and Tees

Nominal diameter, cm (in.)	Screwed				Flanged				
	1.3 (0.5)	2.5 (1.0)	5.0 (2.0)	10 (4.0)	2.5 (1.0)	5 (2.0)	10 (4.0)	20 (8.0)	50 (20)
Valves (fully open):									
Globe	14.0	8.2	6.9	5.7	13.0	8.5	6.0	5.8	5.5
Gate	0.30	0.24	0.16	0.11	0.80	0.35	0.16	0.07	0.03
Swing check	5.1	2.9	2.1	2.0	2.0	2.0	2.0	2.0	2.0
Angle	9.0	4.7	2.0	1.0	4.5	2.4	2.0	2.0	2.0
Elbows:									
45° regular	0.39	0.32	0.30	0.29					
45° long radius					0.21	0.20	0.19	0.16	0.14
90° regular	2.0	1.5	0.95	0.64	0.50	0.39	0.30	0.26	0.21
90° long radius	1.0	0.72	0.41	0.23	0.40	0.30	0.19	0.15	0.10
180° regular	2.0	1.5	0.95	0.64	0.41	0.35	0.30	0.25	0.20
180° long radius					0.40	0.30	0.21	0.15	0.10
Tees:									
Line flow	0.90	0.90	0.90	0.90	0.24	0.19	0.14	0.10	0.07
Branch flow	2.4	1.8	1.4	1.1	1.0	0.80	0.64	0.58	0.41

Figure A3. Loss factor K for valves, elbows, and tees.

Table 7-3 Increased Losses of Partially Open Valves

Condition	Ratio K/K (open condition)	
	Gate valve	Globe valve
Open	1.0	1.0
Closed, 25%	3.0–5.0	1.5–2.0
50%	12–22	2.0–3.0
75%	70–120	6.0–8.0

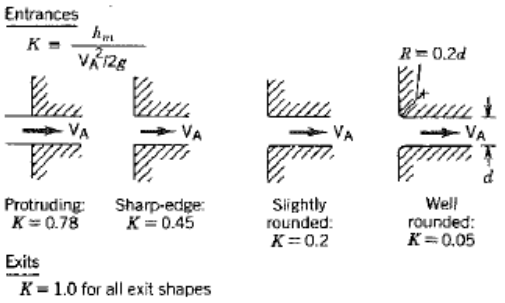

Figure 7-6 Loss factor K for pipe entrances and exits.

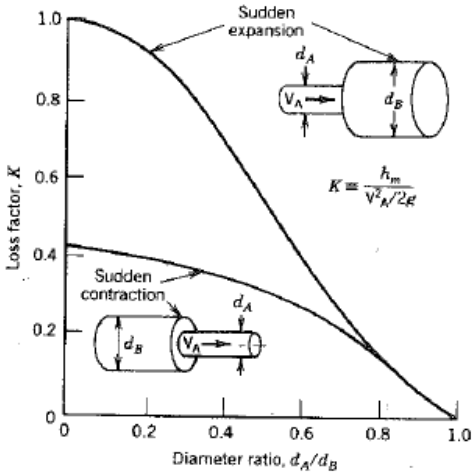

Figure 7-7 Loss factor K for sudden expansions and contractions.

Figure A4. Loss factor K for various components.

Nusselt Correlation Information

From Ref. 10:

$$\mathrm{Nu} = 0.0507\left(X_t^*/X_l^*\right)^{0.2}\left(S/d_o\right)^{0.18}\left(e_f/d_o\right)^{-0.14}\mathrm{Re}^{0.8}\,\mathrm{Pr}^{0.36}\left(\mathrm{Pr}/\mathrm{Pr}_w\right)^{0.25}$$

valid for:

$$2\mathrm{x}10^4 < \mathrm{Re} < 2\mathrm{x}10^5$$
$$1.1 < X_t^* < 4.0$$
$$1.03 < X_l^* < 2.5$$
$$0.06 < S/d_o < 0.36$$
$$0.07 < e_f/d_o < 0.715$$

Variables listed above are defined the following figures:

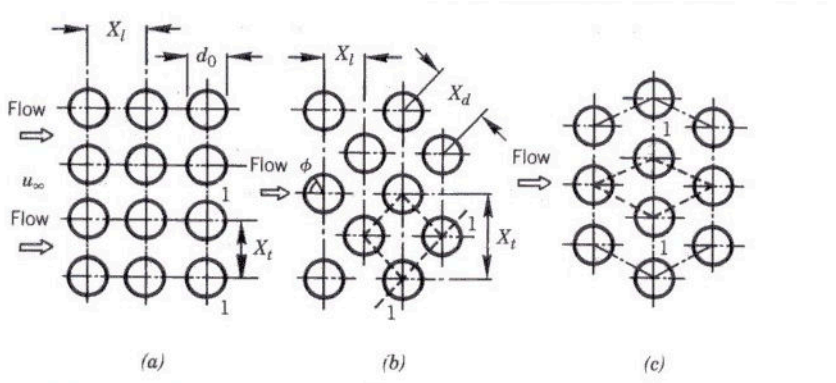

Figure 6.12. Most common types of tube bundle arrangements: (*a*) inline, (*b*)–(*c*) staggered. Minimum intertube spacing at section 1-1 between two tubes.

Figure A5. Tube bundle arrangements (Ref. 10)

The average heat transfer from leading rows of finned tubes in bundles of staggered tube arrangements may be higher or lower than from the inner tubes. Nu_n for short bundles (n < 6) is determined by

$$\mathrm{Nu}_n = c_n \mathrm{Nu}$$

where Nu is the average Nusselt number for a large number of tube rows (n > 6), and c_n is the correction factor depending on the number of rows taken from Figure 6.40 in Ref. 10. For the LSTL, n = 2 tube rows, which corresponds to $c_n = 0.88$.

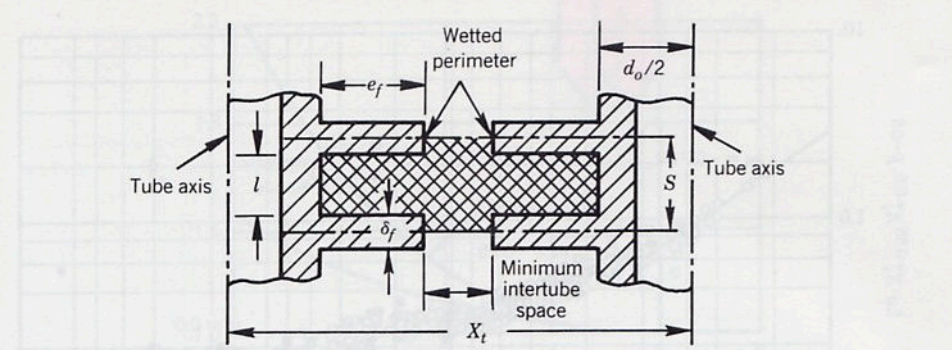

Figure 6.36. Nomenclature for flow over a bank of annular finned tubes. Fluid flow direction is perpendicular to the plane of the paper.

Figure A5. Nomenclature for flow over a bank of annular finned tubes (Ref. 10).

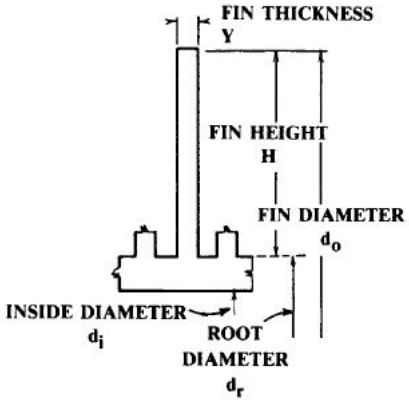

Fig. 1.50 Geometrical Variables for Fin

Figure A6. Geometrical variables for fins.

Vita

Burns Cunningham was born on March 24, 1990. He attended the University of Tennessee and earned his B.S. in Nuclear Engineering in 2012. He continued his education at the University of Tennessee and will earn his M.S. in Nuclear Engineering in 2014. This thesis serves as part of the requirements for graduation from the M.S. program.